Seasonal cycle of averages of nitrous oxide and ozone in the Northern and Southern Hemisphere polar, midlatitude, and tropical regions derived from ILAS/ILAS-II and Odin/SMR observations

F. Khosrawi,[1,2] R. Müller,[3] M. H. Proffitt,[4] J. Urban,[5] D. Murtagh,[5] R. Ruhnke,[6] J.-U. Grooß,[3] and H. Nakajima[7]

Received 31 October 2007; revised 14 May 2008; accepted 28 May 2008; published 20 September 2008.

[1] Northern and Southern Hemispheric monthly averages of ozone (O_3) and nitrous oxide (N_2O) have been suggested as a tool for evaluating atmospheric photochemical models. An adequate data set for such an evaluation can be derived from measurements made by satellites which, in general, have a high spatial and temporal coverage. Here, we use measurements made by the Improved Limb Atmospheric Spectrometers (ILAS and ILAS-II) which use the solar occultation technique and by the Odin-Sub-Millimetre Radiometer (Odin/SMR) which passively observes thermal emissions from the Earth's limb. From ILAS/ILAS-II and Odin/SMR observations, 1-year data sets of monthly averaged O_3 and N_2O, covering a full seasonal cycle, were derived for the latitude range between 60–90°N and 60–90°S, respectively, by partitioning the data into equal bins of altitude or potential temperature. A comparison between both data sets in this latitude region shows a good agreement and verifies that limited sampling from satellite occultation experiments does not constitute a problem for deriving such a full seasonal cycle of monthly averaged N_2O and O_3. Since Odin/SMR provides measurements globally, a 1-year data set of monthly averaged N_2O and O_3 is reported here for both the entire Northern and Southern Hemispheres from these measurements. Further, these hemispheric data sets from Odin/SMR are separated into data sets of monthly averaged N_2O and O_3 for the low latitudes, midlatitudes, and high latitudes. The resulting families of curves help to differentiate between O_3 changes due to photochemistry from those due to transport. These 1-year hemispheric data sets of monthly averaged N_2O and O_3 from Odin/SMR and ILAS/ILAS-II as well as the data sets of monthly averaged N_2O and O_3 for the specific latitude regions from Odin/SMR provide a potentially important tool for the evaluation of atmospheric photochemical models. An example of how such an evaluation can be performed is given using data from two chemical transport models (CTMs), the Chemical Lagrangian Model of the Stratosphere (CLaMS) and the Karlsruhe Simulation Model of the Middle Atmosphere (KASIMA). We find a good agreement between Odin/SMR and the CTMs CLaMS and KASIMA with differences generally less than ±20%.

Citation: Khosrawi, F., R. Müller, M. H. Proffitt, J. Urban, D. Murtagh, R. Ruhnke, J.-U. Grooß, and H. Nakajima (2008), Seasonal cycle of averages of nitrous oxide and ozone in the Northern and Southern Hemisphere polar, midlatitude, and tropical regions derived from ILAS/ILAS-II and Odin/SMR observations, *J. Geophys. Res.*, *113*, D18305, doi:10.1029/2007JD009556.

1. Introduction

[2] Tracer-tracer relationships between long-lived chemical species such as nitrous oxide (N_2O) and ozone (O_3) have been used for several decades to analyze stratospheric data [e.g., *Proffitt et al.*, 1990]. Because of the fact that long-lived tracers tend to exhibit compact, robust relationships in the stratosphere [*Plumb and Ko*, 1992], deviations from such canonical relationships are used to identify chemical and physical processes such as dehydration and denitrification [e.g., *Kelly et al.*, 1989; *Fahey et al.*, 1990; *Rex et al.*, 1999] and ozone loss [e.g., *Proffitt et al.*, 1989a, 1990; *Müller et al.*, 1996; *Salawitch et al.*, 2002; *Tilmes et*

[1]Department of Applied Environmental Science and Department of Meteorology, Stockholm University, Stockholm, Sweden.
[2]Also at ICG-1 and ICG-2, Forschungszentrum Jülich, Jülich, Germany.
[3]ICG-1: Stratosphere, Forschungszentrum Jülich, Jülich, Germany.
[4]Proffitt Instruments Inc., Buenos Aires, Argentina.
[5]Department of Radio and Space Science, Chalmers University of Technology, Göteborg, Sweden.
[6]Institute for Meteorology and Climate Research, Forschungszentrum Karlsruhe, Karlsruhe, Germany.
[7]National Institute of Environmental Studies, Tsukuba, Japan.

0148-0227/08/2007JD009556

al., 2004, 2006b] in the Northern and Southern Hemispheric polar regions. Further, tracer-tracer correlations have been used to determine lifetimes of stratospheric tracers [*Volk et al.*, 1997], descent and mixing [*Ray et al.*, 2002] as well as for determining transport and mixing processes between different latitude regimes [*Volk et al.*, 1996; *Waugh et al.*, 1997]. So far tracer-tracer relations have only been applied to measurements. However, recently ozone-tracer relations have been applied to model data of chemical climate models (CCM) to analyze chemical ozone loss in the polar regions [*Lemmen et al.*, 2006; *Tilmes et al.*, 2007].

[3] *Proffitt et al.* [2003] have suggested a somewhat different way to use tracer-tracer correlations which helps to separate O_3 variability due to latitudinal transport from photochemical changes. In their study, *Proffitt et al.* [2003] consider seasonally averaged lower stratospheric distributions of N_2O and O_3 which were binned by potential temperature or altitude. They suggest these N_2O/O_3 distributions as a valuable tool for the evaluation of atmospheric photochemical models such as Chemical Transport Models (CTMs) and Global Circulation Models (GCMs). The study of *Proffitt et al.* [2003] was based on high-altitude aircraft (ER-2) data obtained during several measurement campaigns, and was restricted to the lower stratosphere and the Northern Hemisphere. In two follow-up studies [*Khosrawi et al.*, 2004, 2006] the method by *Proffitt et al.* [2003] was applied to satellite data derived from the Improved Limb Atmospheric Spectrometers (ILAS/ILAS-II) and extended to the upper stratosphere and to the Southern Hemisphere. However, ILAS/ILAS-II provides only measurements in the polar regions.

[4] Satellite data of N_2O and O_3 as measured by, e.g., the Odin Sub Millimetre Radiometer (Odin/SMR) provide an adequate global data set which can be the basis for such a evaluation study. Here, we compare the combined ILAS/ILAS-II data set [*Khosrawi et al.*, 2006] with a data set derived from Odin/SMR observations. The advantage of the Odin/SMR observation is that measurements are provided for the entire hemisphere and not only for the polar regions as it is the case for ILAS/ILAS-II. Thus, using the Odin/SMR observations we can verify our ILAS/ILAS-II 1-year data set of monthly averaged N_2O and O_3 and extend it to the entire hemisphere as well as to data sets separated into low latitudes, midlatitudes, and high latitudes. Such data sets of monthly averaged N_2O and O_3 are provided here for the first time and constitute a potentially important tool for the evaluation of atmospheric photochemical models. Such kind of tools are presently in demand since differences between models and measurements are still quite large as was shown in the latest model intercomparison by *Eyring et al.* [2006].

2. Data

2.1. ILAS/ILAS-II

[5] The Improved Limb Atmospheric Spectrometers ILAS and ILAS-II were developed by the Ministry of Environment (MOE) and were operated by the Japan Aerospace Exploration Agency (JAXA). ILAS was launched on board the Earth Observing Satellite (ADEOS) on 17 August 1996 and measured continuously from 30 October 1996 to 30 June 1997 [*Sasano et al.*, 1999] while ILAS-II was launched on 14 December 2002 on board ADEOS-II and measured continuously from 2 April 2003 to 24 October 2003 [*Nakajima et al.*, 2006a]. Both instruments used the solar occultation technique which measures the absorption of stratospheric species in the infrared region of solar radiation [*Yokota et al.*, 2002].

[6] The measurements were made in high-latitude regions of the Northern and Southern Hemisphere covering the latitudes from 56°N to 70°N and from 63°S to 88°S (ILAS) and between 54°N to 71°N and 64°S and 88°S (ILAS-II). Measurements of vertical profiles of O_3, HNO_3, NO_2, N_2O, CH_4, H_2O, CFC-11, CFC-12, $ClONO_2$, and N_2O_5 were made 14 times per day in each hemisphere [*Nakajima et al.*, 2006a, 2006b] with a vertical resolution of 1 km. In this study, we use ILAS Version 6.1 [*Nakajima et al.*, 2006b] and ILAS-II Version 1.4 data [*Nakajima et al.*, 2006a]. Validation studies of ILAS Version 5.2 and ILAS-II Version 1.4 ozone data [*Sugita et al.*, 2002, 2006] show a good agreement within ±10% with correlative measurements between 11 and 64 km and between 11 and 40 km, respectively. The validation of ILAS Version 6.1 nitrous oxide data by *Kanzawa et al.* [2002] shows a good agreement with differences less than 20% between 10 and 40 km, ILAS-II Version 1.4 nitrous oxide data show a negative bias of 10% in comparison to the Odin/SMR and balloon-borne measurements [*Ejiri et al.*, 2006]. Nevertheless, this bias is not pronounced in the monthly averages of N_2O and O_3 derived from ILAS-II, and thus, does not seem to have an influence on our results as has been discussed by *Khosrawi et al.* [2006].

2.2. Odin/SMR

[7] The Odin satellite is operated by the Swedish Space Cooperation in cooperation with groups from France, Canada and Finland [*Murtagh et al.*, 2002]. Odin was launched on 20 February 2001 and carries two instruments, the Optical Spectrograph and Infrared Imaging System (OSIRIS) [*Llewellyn et al.*, 2004] and the Sub-Millimetre Radiometer (SMR) [*Frisk et al.*, 2003]. Observations of thermal emission of trace gases originating from the Earth's limb are performed in a time-sharing mode with astronomical observations. In aeronomy mode, various target bands are dedicated to profile measurements of trace constituents relevant to stratospheric and mesospheric chemistry and dynamics such as O_3, ClO, N_2O, HNO_3, H_2O, CO, and NO, as well as isotopes of H_2O and O_3 [e.g., *Murtagh et al.*, 2002; *Merino et al.*, 2002]. Stratospheric mode measurements are performed twice a week. A typical stratospheric mode scan covers the altitude range from 7 to 70 km with a resolution of ≈1.5 km in terms of tangent altitude below 50 km and to ≈5.5 km above. Usually, the latitude range between 82.5°S and 82.5°N is covered by the measurements [*Urban et al.*, 2005a, 2005b].

[8] For the retrieval of vertical profiles from the spectral measurements of a limb scan (aeronomy level 2 processing), two similar data processors have been developed in Sweden and France. Here, we use the Bordeaux V222 data optimized for the retrieval of ClO, N_2O and O_3. A comparison of the V222 O_3 data with data from the Airborne Submillimetre Radiometer (ASUR) shows also a good agree-

ment with differences of −6% to 17% between 20 and 40 km [*Kuttipurath et al.*, 2007]. The validation of N_2O by *Urban et al.* [2005a] shows a relatively good agreement with (not yet validated) N_2O mixing ratios obtained from the ESA Envisat/MIPAS level 2 off-line processor. However, as described in the previous section a comparison with ILAS-II N_2O data show a negative bias of ILAS-II of about 10% compared to Odin/SMR measurements at middle and high latitudes [*Urban et al.*, 2005a; *Ejiri et al.*, 2006].

2.3. KASIMA

[9] The Karlsruhe Simulation Model for the Middle Atmosphere (KASIMA) is a global circulation model including stratospheric chemistry for the simulation of the behavior of physical and chemical processes in the middle atmosphere [*Ruhnke et al.*, 1999; *Reddmann et al.*, 2001]. The meteorological component is based on a spectral architecture with the pressure altitude $z = -H \cdot \ln(p/p_0)$ as vertical coordinate where H = 7 km is a constant atmospheric scale height, p is the pressure, and p_0 = 1013.25 hPa is a constant reference pressure. A horizontal resolution of T42 (2.8° × 2.8°) has been used. In the vertical regime, 63 levels between 10 and 120 km pressure altitude and a 0.75 km spacing from 10 up to 22 km with an exponential increase above were used. The meteorology module of the KASIMA model consists of three versions: the diagnostic model, the prognostic model and the nudged model which combines the prognostic and diagnostic model [*Kouker et al.*, 1999]. For the simulation of the Antarctic vortex split the nudged model version is used. In this version, the model is nudged toward the operational ECMWF analyses of temperature, vorticity and divergence between 18 and 48 km pressure altitude. Below 18 km the meteorology based on ECMWF analyses without nudging, above 48 km pressure altitude the prognostic model has been used. The rate constants of the gas phase and heterogeneous reactions were taken from *Sander et al.* [2003]. The photolysis rates are calculated online with the Fast-J2 scheme of *Bian and Prather* [2002].

2.4. CLaMS

[10] The Chemical Lagrangian Model of the Stratosphere (CLaMS) is a chemistry transport model which simulates the dynamics and chemistry of the atmosphere along trajectories of multiple air parcels [*McKenna et al.*, 2002a, 2002b; *Konopka et al.*, 2004]. CLaMS was initially developed as a two-dimensional model on isentropic surfaces, but further developed into a fully three-dimensional model [*Konopka et al.*, 2004]. The mixing of air parcels, that is the interaction between neighboring air parcels, is introduced both by combining air parcels and adding new air parcels which is driven by the deformation of the flow [*McKenna et al.*, 2002a]. As the air parcels are distributed irregularly in space, the resolution is defined by the mean distance of neighboring air parcels. Here, we used a CLaMS simulation for the Northern Hemisphere with a horizontal resolution of 100 km/300 km north/south of 40°N, respectively [*Grooß et al.*, 2005]. As vertical coordinate potential temperature is used, divided into 30 levels between 350 and 900 K. Vertical motion is calculated as the time derivative of potential temperature using a radiation scheme [*Morcrette*, 1991]. The initialization of O_3 was based on the MIPAS/ENVISAT data from 16 and 17 November 2002.

3. Method

[11] Monthly averages of N_2O and O_3 are calculated by partitioning the data into equal bins of either potential temperature or altitude and averaging within these bins over a fixed interval of N_2O (20 ppbv) [*Proffitt et al.*, 2003; *Khosrawi et al.*, 2004]. For this purpose the potential temperature at the ILAS measurement altitudes was deduced from UK Meteorological office (UKMO) UARS analyses [*Swinbank and O'Neill*, 1994]. To calculate the monthly averages of N_2O and O_3 the data were averaged over potential temperature levels from 350 to 1000 K. By then combining the ILAS and ILAS-II data, a data set covering all seasons was obtained [*Khosrawi et al.*, 2006]. The comparability of these data sets has been established by *Khosrawi et al.* [2006] by comparing the N_2O/O_3 distributions for the months when both instruments were operating.

[12] The resulting data set is used here for the comparison with Odin/SMR data. The months from January to June and November to December are covered by ILAS data and the months from July to October by ILAS-II data. For one entire year (2003) of Odin/SMR data the same method as described above was applied. Since the Odin/SMR data are provided on tangent altitudes, that is on a geometric altitude scale, the data have been interpolated on to potential temperature levels for the binning by potential temperature. For this purpose, fields of, e.g., geopotential height and temperature from the UK Meteorological office (UKMO) meteorological analyses were used. For the comparison of ILAS/ILAS-II data with Odin/SMR data we restricted the calculation of the monthly averages for the Odin/SMR data to the latitudes between 60° and 90° in each hemisphere. This restriction simplifies the comparison between ILAS/ILAS-II and Odin/SMR since ILAS/ILAS II only measured in the high latitudes. However, for the 1-year data set of Odin/SMR we calculated the monthly averages of N_2O and O_3 for the entire hemisphere (0° to 90°N and 0° to 90°S, respectively). Additionally, we separated the 1-year data set of monthly averaged N_2O and O_3 from Odin/SMR into low latitudes, midlatitudes, and high latitudes.

[13] For each averaged data point of N_2O and O_3 the corresponding standard deviations were calculated. Standard deviations for the ILAS/ILAS-II averages are generally around 4–6 ppbv N_2O and 0.1–0.5 ppmv O_3 for the Northern Hemisphere and around 4–6 ppbv N_2O and 0.1–0.3 ppmv O_3 for the Southern Hemisphere. For Odin/SMR the standard deviations for the N_2O averages are similar to the ones derived for ILAS/ILAS-II (5–6 ppbv in the Northern and Southern Hemisphere), but somewhat higher for O_3 for both hemispheres at greater potential temperature levels around 1.5 ppmv above 500 K and between 0.5 and 1 ppmv below. Figures S3 and S4 showing the comparison of ILAS/ILAS-II with Odin/SMR including standard deviations are provided in the auxiliary material[1]. Further, in the auxiliary material, tables containing the data

[1] Auxiliary material data sets are available at ftp://ftp.agu.org/apend/jd/2007jd009556.

for the 1-year data set of monthly averaged N_2O and O_3 derived from Odin/SMR observations are provided.

[14] Our data sets provide a full seasonal cycle of monthly averaged N_2O and O_3 and can be easily used as a tool for the evaluation of atmospheric photochemical models. That is, monthly averages of daily model output of N_2O, O_3, longitude, latitude on a vertical coordinate (potential temperature, altitude or pressure) can be easily compared with our data sets of monthly averaged N_2O and O_3. To test, e.g., if polar ozone destruction is simulated correctly or underestimated or overestimated by the model the corresponding curves (potential temperature levels between 350–450 K) need to be compared with each other. An example for such a evaluation study will be given in section 5.3. For this purpose, we use data from two chemical transport models (CTMs), the CLaMS and KASIMA model. A detailed discussion of the intercomparison will be provided in a separate publication (F. Khosrawi et al., Evaluation of CLaMS, KASIMA and ECHAM5/MESSy1 simulations in the Northern Hemisphere lower stratosphere using observations of Odin/SMR and ILAS/ILAS-II, manuscript in preparation, 2008).

4. Characteristics of the N_2O/O_3 Distribution

4.1. Influence of Limited Sampling on the N_2O/O_3 Distribution

[15] *Sankey and Shepherd* [2003] employed the Canadian Middle Atmosphere Model (CMAM) and plotted correlations of various chemical species to investigate the conditions under which compact correlations can be expected to be formed. Their analysis also served as validation of the model results. *Sankey and Shepherd* [2003] showed that the correlations produced by the CMAM agree well with the theory of *Plumb and Ko* [1992]. They raise the question whether limited sampling from satellite occultation experiments or aircraft data could lead to artificially compact correlations. In our study we will show that ILAS/ILAS-II and Odin/SMR measurements provides data sets with a high sampling frequency and thus with a high spatial and temporal resolution. Further, we do not consider the correlation of N_2O and O_3 itself since we use monthly averages of N_2O and O_3 and consider N_2O/O_3 relations on altitude and potential temperature levels, respectively.

[16] In a previous study *Khosrawi et al.* [2004] comparing monthly averaged O_3 and N_2O derived from ILAS with monthly averaged O_3 and N_2O derived from ER-2 data by *Proffitt et al.* [2003] a good agreement was found though both data sets were derived from different kinds of limited sampling. *Proffitt et al.* [2003] used in situ measurements from the ER-2 over a time period of 8 years covering the Northern Hemisphere from the tropics to the polar regions while the ILAS remote sensing data used by *Khosrawi et al.* [2004] covered the polar regions continuously for a time period of 8 months. A good agreement was also found between ILAS and ILAS-II for the months where measurements from both instruments were available [*Khosrawi et al.*, 2006]. Further, as will be shown in this study, good agreement between ILAS/ILAS-II and Odin/SMR is found, wherever measurements are available over the entire hemisphere, demonstrating that limited sampling of the ILAS and ILAS-II occultation instruments does not constitute a problem in our analyses. Furthermore, since data from different years were used for these comparison we could also show that differences between different years were small in the monthly averages of O_3 and N_2O.

[17] The only effect which can be found in the monthly averages of N_2O and O_3 resulting from limited sampling of ILAS and ILAS-II is a smaller extension of the curves in the N_2O range (which however is dependent on season and the air masses measured). To make this point more clearly, if one considers the reference curves of the N_2O/O_3 distribution in the tropics and midlatitudes one will find that the families of curves connect these reference curves (at each potential temperature level). Whether our curves reach exactly to the reference curves in the tropics is dependent on the fact whether tropical air is measured by ILAS or ILAS-II. Since this is not the case for ILAS and ILAS-II, these curves will have a lesser extension in the N_2O range.

4.2. Influence of Dynamics on the O_3/N_2O Distribution

[18] Radiative cooling inside the polar vortex leads to subsidence across isentropic surfaces or diabatic descent of the vortex column air by several kilometers [e.g., *Proffitt et al.*, 1989b; *Tuck*, 1989; *Murphy et al.*, 1989; *Schoeberl and Hartmann*, 1991; *McIntyre*, 1992]. Several quantitative studies of vortex descent have been carried out in the past and descent has been inferred both in the Arctic [e.g., *Bauer et al.*, 1994; *Greenblatt et al.*, 2002; *Ray et al.*, 2002] and Antarctic [e.g., *Russell et al.*, 1993a, 1993b; *Kawamoto et al.*, 2004]. Further, models have also been used to estimate descent [e.g., *Rosenfield et al.*, 1994; *Strahan et al.*, 1999]. Measurements as well as model studies have shown that in the polar regions air is drawn down from a large range of altitudes (including the entire depth of the mesosphere) into the polar stratosphere [*Danielsen and Houben*, 1988; *Bacmeister et al.*, 1995; *Ray et al.*, 2002; *Plumb et al.*, 2002; *Engel et al.*, 2006]. The most rapid descent at high latitudes occurs at the higher altitudes of the stratosphere during the Northern Hemispheric fall and early winter [*Rosenfield et al.*, 1994].

[19] Stratospheric tracers such as N_2O are ideal for studies of polar descent within the stratosphere. N_2O is chemically long lived with a lifetime of many years below 30 km at midlatitudes; it has a source in the troposphere and a photochemical sink in the middle and upper stratosphere [e.g., *Solomon et al.*, 1986]. Therefore, mean N_2O mixing ratios decrease with increasing altitude in the stratosphere. This gradual decrease of N_2O with increasing altitude is due to N_2O photodissociation in the middle and upper stratosphere and the vertical profile at a particular location is the result of transport and mixing of air between the source and sink regions. In situ measurements by *Strahan et al.* [1999] made by the Airborne Tunable Laser Absorption Spectrometer (ATLAS) have shown that in the lower stratosphere the zonally averaged N_2O mixing ratios vary systematically with season, latitude and altitude. They also showed that local changes from the seasonal zonal mean profile can be interpreted as the result of recent stratospheric transport. As pointed out in earlier work [e.g., *Müller et al.*, 1996; *Ray et al.*, 2002; *Sankey and Shepherd*, 2003] descent itself will not change tracer-tracer correlation curves. However, using the method proposed by *Proffitt et al.* [2003] calculating monthly averages of O_3 and N_2O by partitioning the data

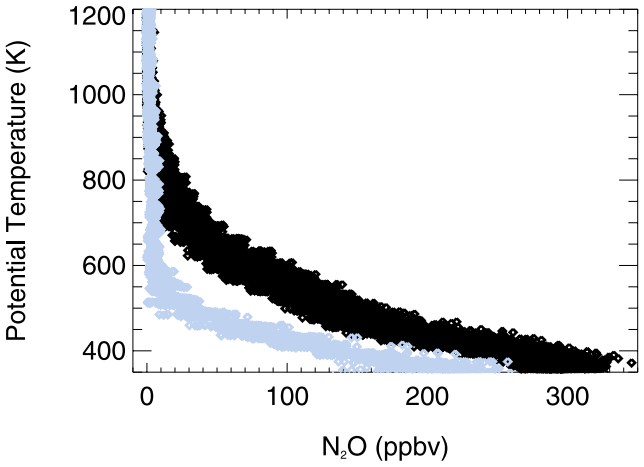

Figure 1. Southern Hemispheric N_2O measured by ILAS-II versus potential temperature derived from UKMO analyses in April (black diamonds) and September (gray diamonds).

into bins of potential temperature or altitude and then averaging over a fixed interval of N_2O helps to separate dynamical and chemical processes, making the effects of descent on the families of curves visible [*Proffitt et al.*, 2003; *Khosrawi et al.*, 2004, 2006].

[20] Therefore, changes in the families of curves of O_3/N_2O as they are discussed here are not only caused by chemical ozone loss or production, but also by transport processes. How diabatic descent influences N_2O can be seen from the resulting relationship of N_2O and potential temperature. In Figure 1, ILAS-II N_2O versus potential temperature is shown for April and September in the Southern Hemisphere. In April the strength of the diabatic descent begins to increase and the relationship between N_2O and potential temperature is curved. This is in contrast to January (not shown) where descent is weak and an almost linear relationship is found. However, in September only very low N_2O mixing ratios are observed above 500 K (generally below 20 ppbv). The larger N_2O mixing ratios are only found below 500 K (greater than 20 ppbv). The low N_2O mixing ratios at greater altitudes are due to photochemical loss of N_2O and are transported downward by diabatic descent during winter.

[21] The above relationship between N_2O and potential temperature is also reflected in the N_2O/O_3 distributions. In

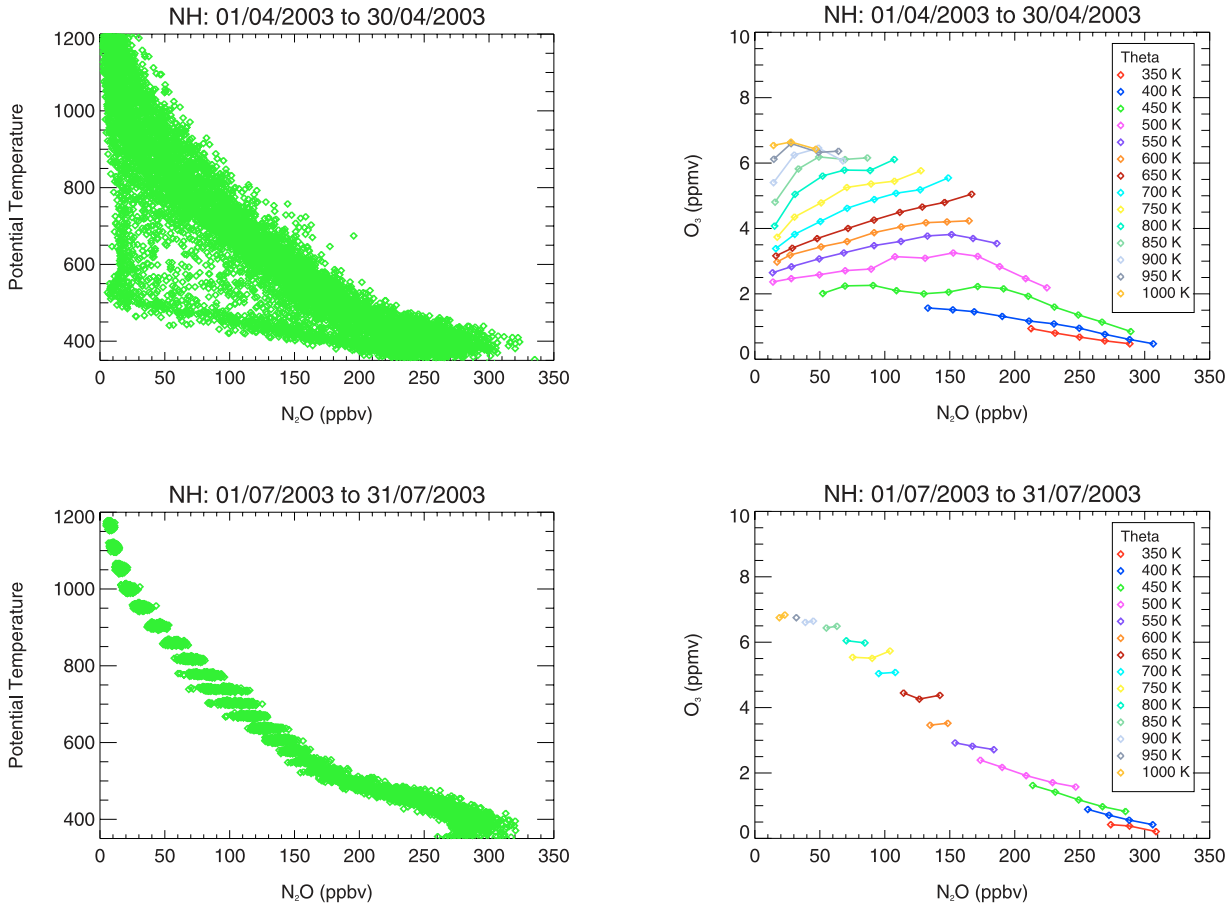

Figure 2. Northern Hemispheric N_2O measured by ILAS-II versus potential temperature derived from UKMO analyses in (top left) April and (bottom left) July. Northern Hemispheric monthly averages of N_2O and O_3 derived from ILAS-II measurements binned by potential temperature for (top right) April and (bottom right) July.

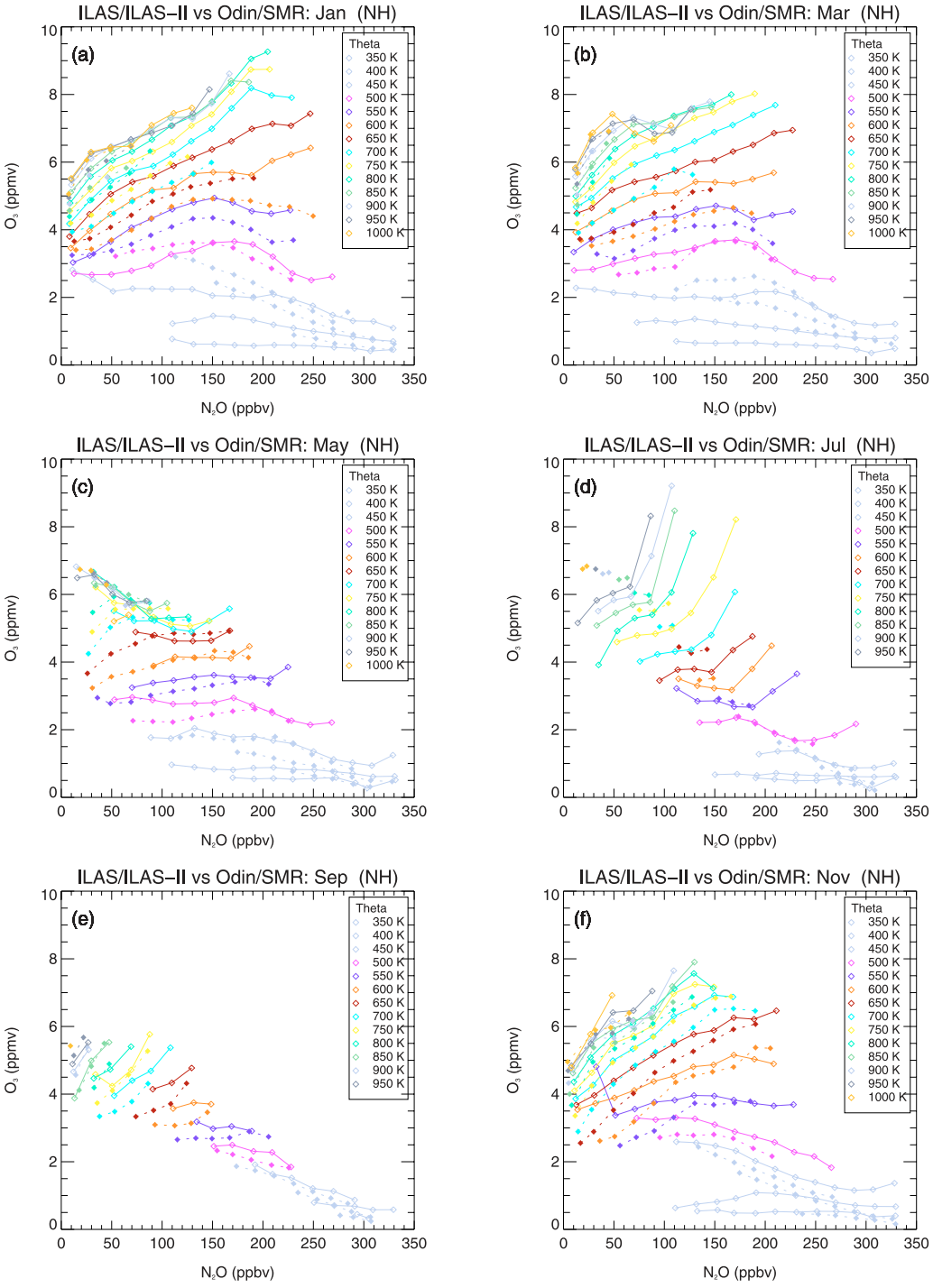

Figure 3. Northern Hemispheric monthly averaged N_2O and O_3 measured by Odin/SMR (solid lines) and ILAS/ILAS-II (dashed lines) binned by potential temperature (ILAS, 56–70°N; ILAS-II, 54–71°N; Odin/SMR, 60–90°N). (a–c) January to May, ILAS versus Odin/SMR; (d and e) July to September, ILAS-II versus Odin/SMR; and (f) November, ILAS versus Odin/SMR.

Figure 2 (left) N_2O versus potential temperature is shown for April and July in the Northern Hemisphere. The corresponding averages of N_2O and O_3 are shown in Figure 2 (right). In April low values of N_2O are found at all levels above 500 K because of diabatic descent as well as higher N_2O values from outside the polar vortex resulting in a broad distribution of N_2O versus potential temperature (Figure 2, left). In the averages this is reflected by N_2O/O_3 curves which extend over a broad range of N_2O mixing ratios and which exhibit a positive correlation (increasing N_2O with increasing O_3) above 500 K (Figure 2, right). In July, when descent is weak a compact but slightly curved relationship is found. A weak descent results in quasi-horizontal mixing time scales to be short enough to establish a rather uniform polar average at a given potential temperature level. That is, N_2O increases with potential tempera-

ture and extends over a very narrow N_2O range at each potential temperature (Figure 2, bottom left). This is reflected in the families of curves of N_2O/O_3 by a flat to negative correlation of the N_2O/O_3 curves at all levels and by a confinement of the N_2O/O_3 relation to a narrow range of N_2O mixing ratios at each potential temperature level (Figure 2, bottom right).

5. Results

5.1. ILAS/ILAS-II Versus Odin/SMR

[22] For the comparison of the Odin/SMR 1-year data set with the ILAS/ILAS-II 1-year data set the monthly averages of N_2O and O_3 derived from the Odin/SMR measurements were restricted to the latitudes between 60° to 90°. The monthly averages of N_2O and O_3 for the Northern and Southern Hemisphere were calculated as described in section 3. To present the results more concisely only every second month is shown in Figures 3 and 4. The months from January to May and November are covered by ILAS and the months from July to September by ILAS-II. Despite the spatial and temporal differences of the data sets (Odin measures every third day the entire hemisphere while ILAS/ILAS-II measures every day at a narrow latitude band) a good agreement between Odin/SMR and ILAS/ILAS-II is found in both hemispheres, demonstrating that the limited spatial sampling from solar occultation satellites does not constitute a problem for deriving a full seasonal cycle of monthly averaged N_2O and O_3. This means that mixing must be strong enough to homogenize the air masses in a way so that a limited (solar occultation) sampling is sufficient to characterize the air masses in question. This is consistent with the results of *Hegglin and Shepherd* [2007] who assess the representativeness of the Atmospheric Chemistry Experiment (ACE) satellite measurements, which is also a solar occultation instrument, by comparing these data with data from the Canadian Middle Atmosphere Model (CMAM). Solely, below 500 K larger differences are found between Odin/SMR and ILAS/ILAS-II. However, at these levels the Odin/SMR measurements are flawed by a low measurement response and are thus not reliable. To emphasize this fact we show them colored in gray (Figures 3–12). Further, to avoid confusion and keep Figures 3–12 more concise also the ILAS/ILAS-II curves below 500 K are colored in gray.

5.1.1. Northern Hemisphere

[23] The monthly averages of N_2O and O_3 binned by potential temperature (350 to 1000 K, $\Delta\Theta$ = 50 K) derived from Odin/SMR and ILAS/ILAS-II are shown for every second month (January to November) in Figure 3. Above 500 K at all potential temperature levels a positive correlation (increasing N_2O with increasing O_3) is found while at the levels below a negative (ILAS/ILAS-II) to flat correlation (Odin/SMR) is found. The positive correlation above 500 K is caused by descent which brings down air from above the O_3 maximum that is characterized by lower O_3 and N_2O mixing ratios [*Proffitt et al.*, 2003; *Khosrawi et al.*, 2004, 2006]. An exception is May (Figure 3c) and June (not shown) where a negative to flat correlation is found at all potential temperature levels.

[24] From January to March (Figures 3a and 3b) photochemical ozone destruction is evident at 450 ± 25 K to 500 ± 25 K by a gradual change of slope with an inflection at 190 ppbv (Odin/SMR) and 150 ppbv (ILAS/ILAS-II) N_2O in January (500 ± 25 K). Previous studies have reported evidence for chlorine-catalyzed photochemical ozone destruction in the lower Arctic stratosphere during late winter and early spring based on observations and model results [e.g., *Browell et al.*, 1990; *Salawitch et al.*, 1990; *McKenna et al.*, 1990] and for the winters 1997 and 2003 based on model results [e.g., *McKenna et al.*, 2002b; *Goutail et al.*, 2005; *Grooß et al.*, 2005] and satellite observations [e.g., *Pierce et al.*, 1997; *Tilmes et al.*, 2003b; *Urban et al.*, 2004; *Müller et al.*, 2007]. The difference in the location of the inflection is probably due to differences between the winters 1996/1997 and 2002/2003. However, we cannot exclude that to some extent also instrumental or sampling differences contribute to this difference. Estimations of ozone loss from HALOE measurements and ILAS-II [*Tilmes et al.*, 2004; *Müller et al.*, 2007] as well as from SAOZ measurements and the REPROBUS model [*Goutail et al.*, 2005] show a reduction in total ozone column due to chemical O_3 loss for the winter of 2002/2003 comparable to that for the winter 1996/1997. However, in the winter of 2002/2003 the vortex was characterized by very low temperatures in the early vortex and chlorine activation already in mid-December [*Tilmes et al.*, 2003a; *Urban et al.*, 2004].

[25] Toward May (Figure 3c), when descent is weak, the families of curves begin to flatten and the correlation changes to negatively correlated in the upper levels. Even after the breakup of the vortex, remnants of polar vortex air (low O_3 and N_2O) can be found at lower levels (450–550 K) in April and May. Somewhat more remnants of vortex air are found in the Odin/SMR data which is again due to differences in the ozone chemistry in the winters 1996/1997 and 2002/2003. In the dynamically active winter of 2002/2003, the time when the vortex was exposed to sunlight began earlier and was longer than in other winters [*Grooß et al.*, 2005]. By July (Figure 3d) the remnants of vortex air have completely mixed with the midlatitude air and the low values of O_3 and N_2O between 450 ± 25 K and 550 ± 25 K have disappeared. Summer O_3 loss due to NO_x-catalyzed O_3 loss cycles is expected to occur with increasing intensity from May on [*Farman et al.*, 1985b; *Pierce et al.*, 1999; *Toon et al.*, 1999; *Crutzen and Brühl*, 2001]. In the families of curves summer O_3 loss can be seen as a general decline of O_3 between May (Figure 3c) and August (not shown) at levels above 550 K.

[26] Descent appears as a positive correlation at the uppermost potential temperature levels in July (Figure 3d) and continuous gradually through November down to 700 K (Figure 3f). This feature is more pronounced in the Odin/SMR data since Odin/SMR measurements cover a larger part of the polar region (measurements between 60 and 90°N are shown) while ILAS measurements where made at that time at midlatitudes (≈50°N). Descent brings down air characterized by low O_3 and N_2O and leads to a positive correlation in the upper potential temperature levels (above 500 K). Strong descent results in a steepening of the positively correlated curves. Thus, the stronger the descent the stronger the steepening [*Khosrawi et al.*, 2004]. For a constant value of nitrous oxide an increase in O_3 with potential temperature can be found below the O_3 maximum (≈30 km) in each of the monthly families of curves. This

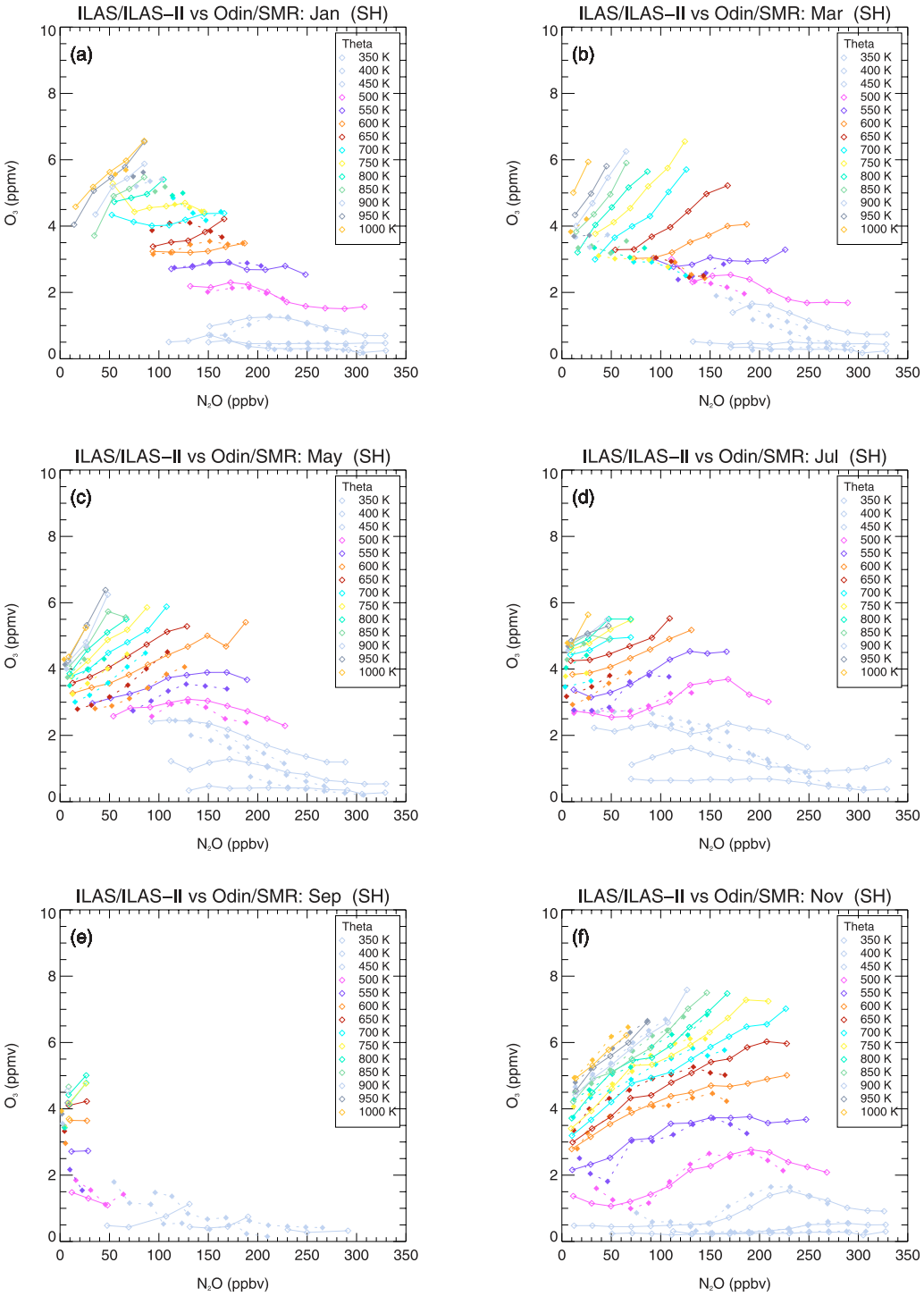

Figure 4. Southern Hemispheric monthly averaged N_2O and O_3 measured by Odin/SMR (solid lines) and ILAS/ILAS-II (dashed lines) binned by potential temperature (ILAS, 63–88°; ILAS-II, 64–88°S; Odin/SMR, 60–90°S). (a–c) January to May, ILAS versus Odin/SMR; (d and e) July to September, ILAS-II versus Odin/SMR; and (f) November to December, ILAS versus Odin/SMR.

dependence was termed "O_3-Θ dependence" [*Proffitt et al.*, 1990, 1993, 2003]. Within the Arctic vortex and below 500 K this dependence cannot solely be explained by descent from above the O_3 maximum. The "O_3-Θ dependence" also requires photochemical winter loss of O_3 in the presence of diabatic cooling [*Proffitt et al.*, 2003].

5.1.2. Southern Hemisphere

[27] Summer ozone loss due to NO_x catalyzed chemical cycles [e.g., *Crutzen*, 1970; *Johnston*, 1975; *Farman et al.*, 1985b; *Crutzen and Brühl*, 2001] is evident from January to March by a general decline of ozone at potential temperature levels above 550 K (Figures 4a and 4b). The summer

ozone loss is more pronounced in the families of curves derived from ILAS/ILAS-II than in the families of curves derived from Odin/SMR. Clearly, the differences are caused by the fact that Odin/SMR measures a greater amount of midlatitude air even though differences of the summer photochemistry in the years 1997 and 2003 cannot be excluded. With the formation of the polar vortex in April (not shown) and the associated diabatic descent in the polar vortex region the curves exhibit a steep slope with a positive correlation in the upper potential temperature levels and a negative correlation in the lower levels. This characteristic is found in the Odin/SMR data already in March (Figure 4b) and in the ILAS/ILAS-II data somewhat later, namely in April (not shown). This difference between ILAS/ILAS-II and Odin/SMR is caused by differences in the years 1997 and 2003. The evolution of the vortex in March 1997 was different from 2003 though the vortex in both Antarctic winters started forming in March [*Tilmes et al.*, 2006a]. The vortex in March 1997 was smaller than the vortex in 2003.

[28] Evidence for chemical ozone loss in the Antarctic during late winter and early spring has been reported since the mid-1980s on the basis of observations. Strong chemical ozone depletion was first documented in the Antarctic spring by *Farman et al.* [1985a] on the basis of measurements at the British Arctic survey station at Halley. Remote measurements were later confirmed with in situ aircraft observations out of Punta Arenas, Chile [e.g., *Anderson et al.*, 1989; *Proffitt et al.*, 1989a, 1989b, 1989c, 1989d]. Many studies followed giving evidence for ozone loss in the Antarctic during subsequent winters and ozone loss rates were estimated to quantify ozone depletion, e.g., for the winter 1987 by *Murphy* [1991]. Further studies, e.g., by *Tuck et al.* [1995] showed that significant ozone loss occurs below 500 K between June and August.

[29] The levels below 450 K remain almost unchanged from May to July (Figures 4c and 4d). In the levels above 450 K descent is becoming less pronounced. In July at 500 ± 25 K, polar ozone loss is indicated by an inflection and thus a change of slope. In fact, *Tilmes et al.* [2006b] found on the basis of ILAS-II measurements significant deviations from the early winter reference in mid-July 2003 thus indicating severe chemical ozone loss. In the ILAS/ILAS-II data the inflection is found at 100 ppbv N_2O and in the Odin/SMR data the inflection is found at 170 ppbv N_2O. This difference in the inflection is due to the fact that the Odin/SMR data have a stronger influence from midlatitude air. That is, during that period, Odin/SMR measures the entire hemisphere while ILAS/ILAS-II measures over a limited range near 70°S. Very low ozone values are observed by ILAS/ILAS-II and Odin/SMR from September to November at potential temperature levels between 450 and 550 K (Figures 4e and 4f). At 500 ± 25 K somewhat lower ozone values were observed by Odin/SMR than by ILAS/ILAS-II. In September the minimum is found at O_3 values around 1 ppmv between 10 and 60 ppbv N_2O (ILAS/ILAS-II) and 10 to 90 ppbv N_2O (Odin/SMR), respectively. This difference is also likely due to the fact that Odin/SMR measured more midlatitude air than ILAS/ILAS-II since the Odin/SMR measurements discussed here cover the entire latitude range from 60°S to 90°S. The minima of O_3 remain in November (Figure 4f) and December (not shown) but with somewhat higher O_3 mixing ratios than in September (Figure 4e). In November the families of curves exhibit again a pronounced positive correlation at levels above 500 K. In November, these minima are more pronounced in the ILAS/ILAS-II data which is due to the fact that ILAS/ILAS-II mostly measures inside the polar vortex while Odin/SMR measures also a certain amount of air from outside the vortex (Figure 4f).

5.2. Odin/SMR N_2O/O_3 Distributions

[30] In the following a 1-year data set of monthly averaged N_2O and O_3, thus, a full seasonal cycle, derived from Odin/SMR for the entire Northern Hemisphere (0° to 90°) and Southern Hemisphere (0° to −90°) will be presented. To make the presentation more concise only every second month is shown (Figures 5 and 6). The entire seasonal cycle of monthly averaged N_2O and O_3 (showing every month, thus the entire year) as well as tables containing all averaged data points of the N_2O and O_3 distribution including standard deviations are provided as auxiliary material. The May midlatitude (ATMOS Shuttle 1985 [*Proffitt et al.*, 1990]), April high-latitude (ATMOS Shuttle 1993 [*Michelsen et al.*, 1998]) and November tropics (ATMOS Shuttle 1994 [*Michelsen et al.*, 1998]) reference curves are included in Figures 5 and 6 to help identifying air of tropical and air of polar character [*Proffitt et al.*, 2003; *Khosrawi et al.*, 2004]. Further, the 1-year data set of monthly averaged N_2O and O_3 separated into low latitudes, midlatitudes and high latitudes is shown in Figures 7, 9, and 11 for the Northern Hemisphere and in Figures 8, 10, and 12 for the Southern Hemisphere.

[31] The major difference between the families of curves covering the entire latitude range and the ones restricted to 60° to 90°N and 60° to 90°S, respectively, is that the former extend over a larger N_2O range, including also greater N_2O mixing ratios, which is mainly due to the inclusion of tropical air (Figures 7 and 8). While polar summer (general decline of ozone with potential temperature) and polar winter ozone loss (change of slope from negatively to positively correlated) are pronounced in the families of curves, descent (positive correlation above 500 K) is less pronounced. The characteristics of descent at high latitudes is masked because of the inclusion of tropical air. Further, the change of slope to negative or flat correlated at all potential temperature levels is also not pronounced in the families of curve when the entire latitude range is considered. As discussed in section 5.1 the levels below 500 K are not reliable because of a too low measurement response which is emphasized by coloring these curves in gray (Figures 5–12).

5.2.1. Northern Hemisphere

[32] A positive correlation is found at the levels above 650 K throughout the year (Figure 5). The N_2O values which show mixing ratios greater than the November tropics reference curve can be attributed to air of tropical origin (Figure 7). Throughout the year, O_3 is produced primarily in the tropical stratosphere where peak production rates occur at altitudes near 30 km during equinox, and minimum rates occur during solstice [*Perliski et al.*, 1989]. The highest ozone values are found in March (Figure 5b) with O_3 values of up ≈12 ppmv at N_2O values between 250 and 350 ppbv. These maximum values are in agreement with the maximum values of the O_3 climatology derived

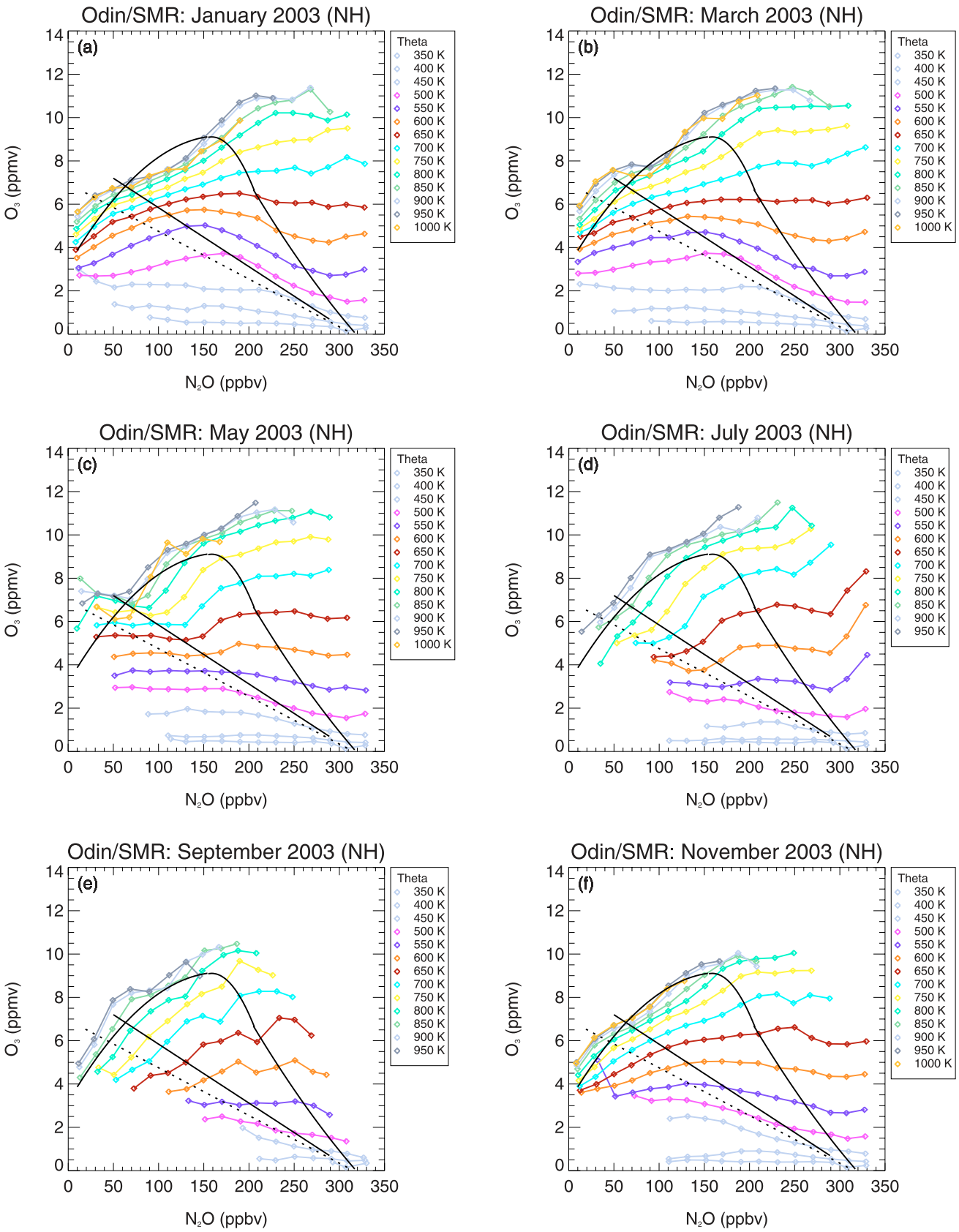

Figure 5. Northern Hemispheric monthly averaged N_2O and O_3 measured by Odin/SMR binned by potential temperature (Odin/SMR, 0–90°N). Additionally, the May midlatitude (ATMOS Shuttle 1985, solid line), April high-latitude (ATMOS Shuttle 1993, dashed line), and November tropics (ATMOS Shuttle 1994, solid curve) reference curves are shown.

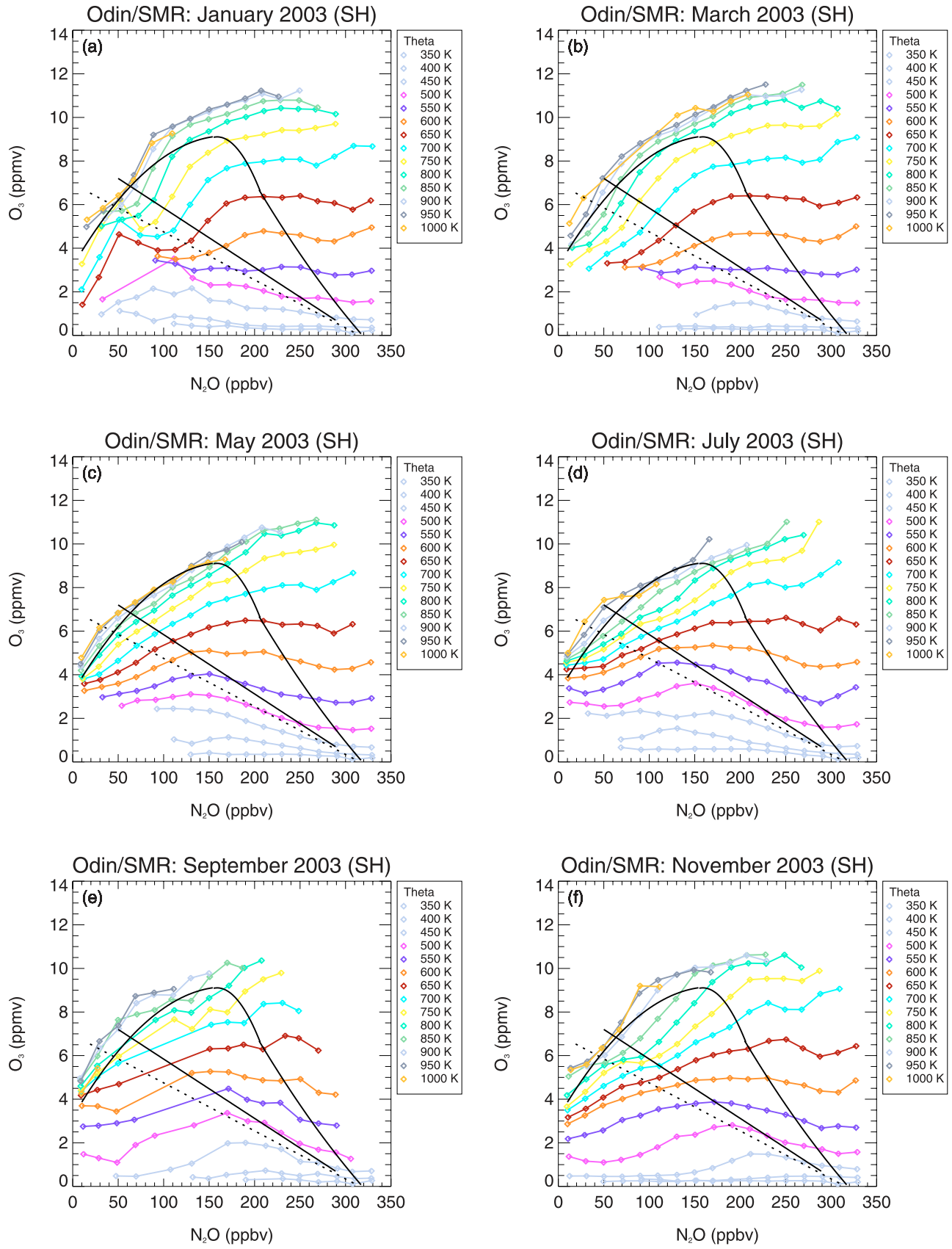

Figure 6. Southern Hemispheric monthly averaged N_2O and O_3 measured by Odin/SMR binned by potential temperature (Odin/SMR, 0–90°S). Additionally, the May midlatitude (ATMOS Shuttle 1985, solid line), April high-latitude (ATMOS Shuttle 1993, dashed line), and November tropics (ATMOS Shuttle 1994, solid curve) reference curves are shown.

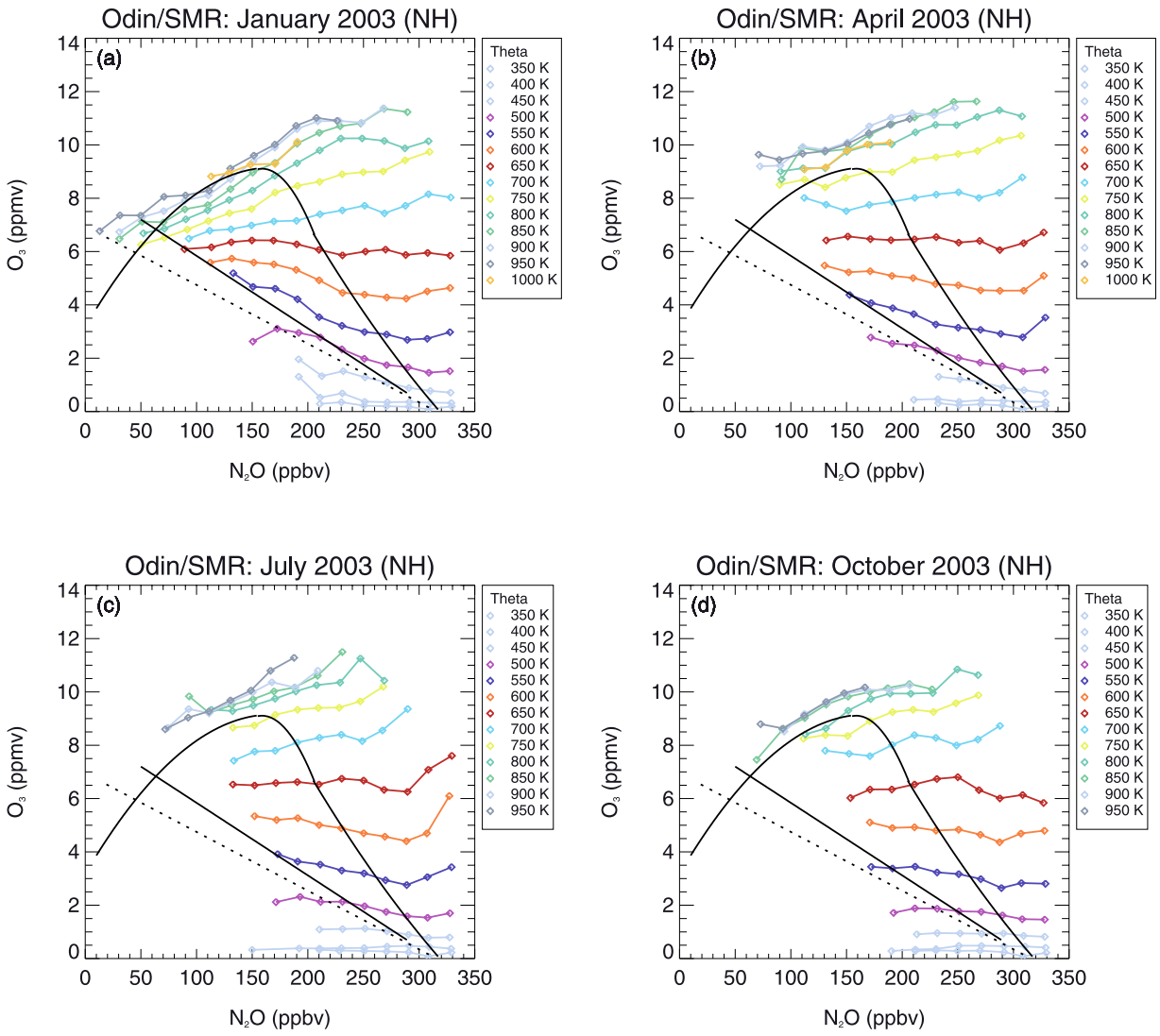

Figure 7. Northern Hemispheric monthly averaged N_2O and O_3 for the low latitudes measured by Odin/SMR binned by potential temperature (Odin/SMR, 0–30°N). Additionally, the May midlatitude (ATMOS Shuttle 1985, solid line), April high-latitude (ATMOS Shuttle 1993, dashed line), and November tropics (ATMOS Shuttle 1994, solid curve) reference curves are shown.

from HALOE observations [*Grooß and Russell*, 2005]. Ongoing winter ozone destruction is evident at 450 K and 500 K from January to March by a gradual slope change from positive to negative with an inflection at 190 ppbv in January (Figures 5a and 7a).

[33] After the breakup of the polar vortex in April remnants of polar vortex air (low N_2O and low O_3) are still found in April (not shown) and May (Figure 5c). That these values can be attributed to polar air can be seen from Figure 11b. These low values are completely removed through mixing with midlatitude air by June (not shown). Summer polar ozone loss is evident in July and August by a general decline of O_3 at levels above 550 K (Figures 5d and 11c). In May, when descent is weak a flat correlation is found at all potential temperature levels for N_2O values lower than the midlatitude reference curve. Starting in July descent is increasing and brings down air with low N_2O and O_3 mixing ratios which are particularly pronounced in November (Figure 5f) at N_2O values lower than 50 ppbv.

5.2.2. Southern Hemisphere

[34] As in the Northern Hemisphere, a positive correlation is found throughout the year at all potential temperature levels above 700 K. Summer polar ozone loss is evident above 550 K from January to March by a general decline of ozone (Figures 6a and 6b). From April (not shown) to July (Figure 6d) the N_2O/O_3 relations at potential temperature levels above 650 K remain almost unchanged while winter polar ozone loss becomes evident beginning in July at potential temperature levels between 450 ± 25 K and 550 ± 25 K (Figures 6d and 12c). The families of curves change their slope from positive to negative correlated and at 500 ± 25 K the inflection is found at 150 ppbv N_2O (July).

[35] Very low ozone values are observed from September (Figure 6e) to December (not shown). Because of the prior ozone destruction, the lowest ozone values are found in October (not shown) at 500 ± 25 K with O_3 values around 0.5 ppmv. In November (Figure 6f) and December (not

Tropics (SH)

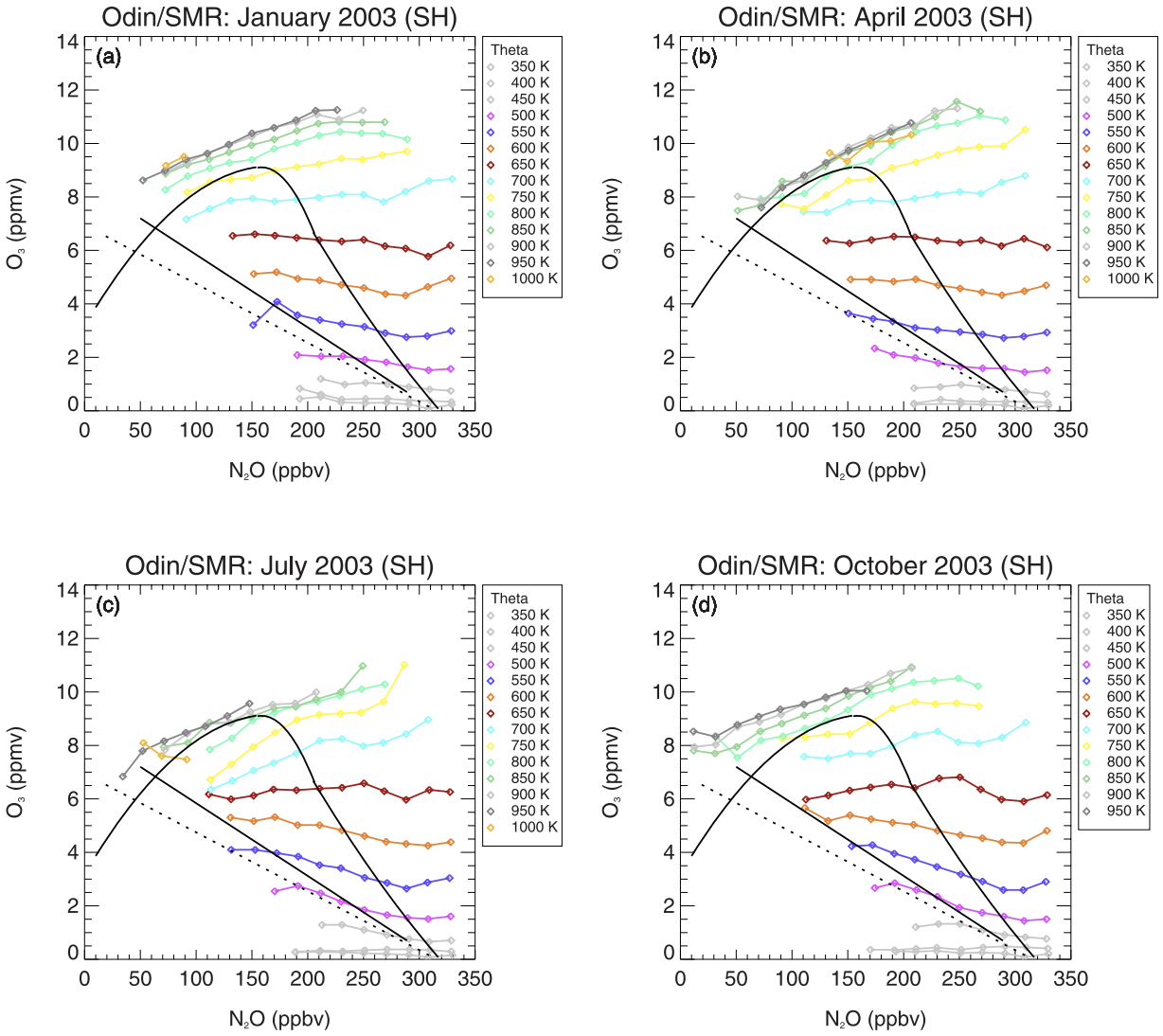

Figure 8. Southern Hemispheric monthly averaged N_2O and O_3 for the low latitudes measured by Odin/SMR binned by potential temperature (Odin/SMR, 0–30°S). Additionally, the May midlatitude (ATMOS shuttle 1985, dashed line), April high-latitude (ATMOS Shuttle 1993, dashed line), and November tropics (ATMOS shuttle 1994, solid curve) reference curves are shown.

shown) ozone values remain low, but start increasing slightly after the final warming and breakup of the polar vortex due to dilution with midlatitude air. Further, owing to the same reason a slight ozone decrease can be found at midlatitudes (values which are centered around the midlatitude reference curves).

5.2.3. Separation Into High, Middle, and Low Latitudes

[36] The separation into low latitudes, midlatitudes, and high latitudes shows that the tropics are not truly isolated from midlatitudes and that these are not truly isolated from the high latitudes [e.g., *Tuck*, 1989; *Proffitt et al.*, 1989b, 2003; *Tuck and Proffitt*, 1997; *Randel et al.*, 1993; *Michelsen et al.*, 1998]. Data taken well outside the tropics can be of tropical character [*Randel et al.*, 1993]. However, in general the tropical air has N_2O mixing ratios that are greater than the midlatitude and tropic reference curve while the midlatitude air is centered around the midlatitude reference curve and the high-latitude air has N_2O mixing ratios that are lower than the midlatitude and high-latitude reference curves.

[37] The separation of the data set of monthly averaged N_2O and O_3 into high latitudes, midlatitudes, and low latitudes reveals the rather different characteristics of the O_3/N_2O distribution of these air masses. In the tropics (Figures 7 and 8), the O_3/N_2O distribution is characterized by N_2O values higher than the May midlatitude and November tropics reference curves. A flat to positive correlation is found at potential temperature levels above 700 K (Northern and Southern Hemisphere). The positive

Midlatitude (NH)

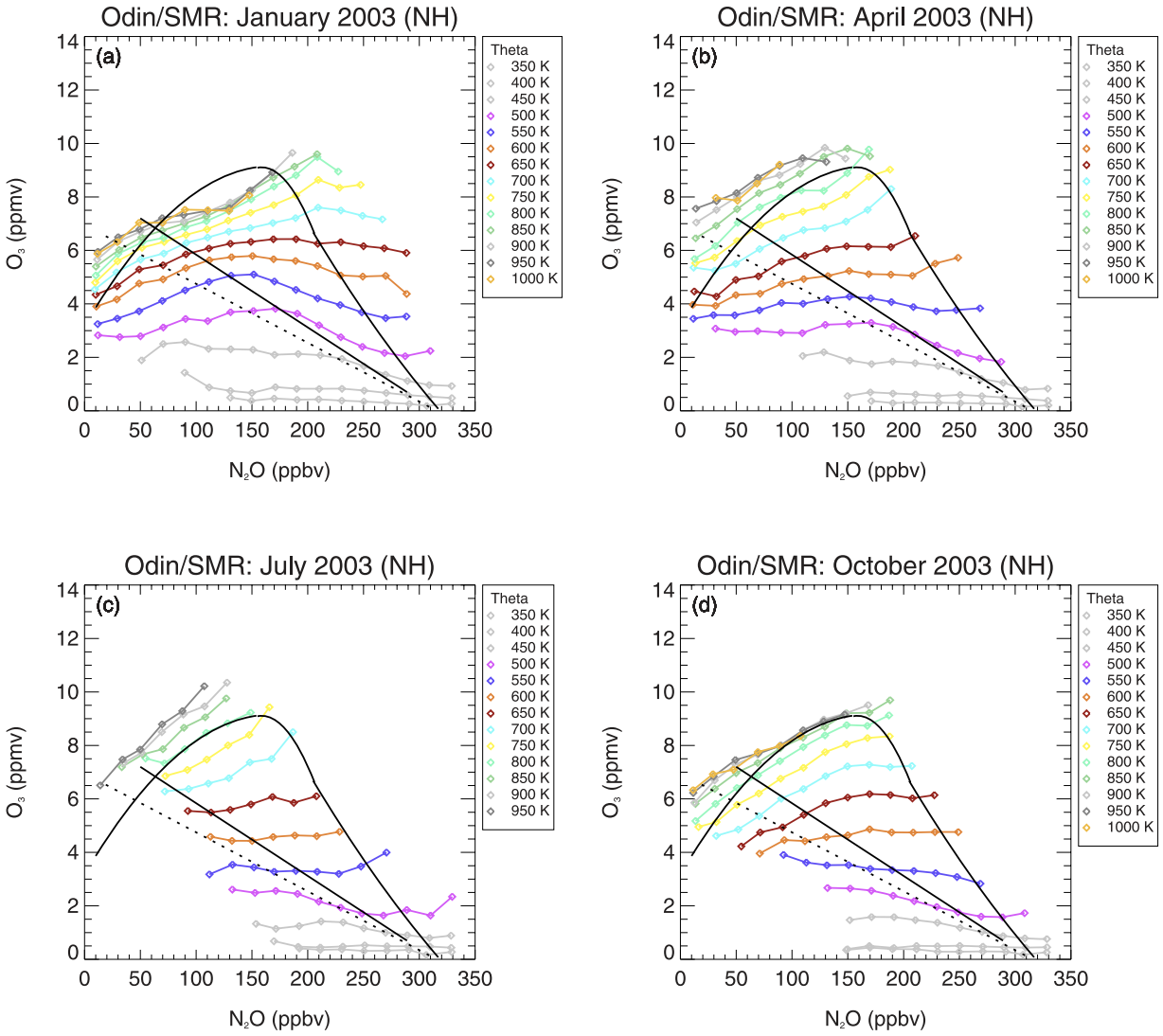

Figure 9. Northern Hemispheric monthly averaged N_2O and O_3 for the midlatitude measured by Odin/SMR binned by potential temperatures (Odin/SMR, 30–60°N). Additionally, the May midlatitude (ATMOS shuttle 1985, solid line), April high-latitude (ATMOS Shuttle 1993, dashed line), and November tropics (ATMOS Shuttle 1994, solid curve) reference curves are shown.

correlation is caused by the photochemical production of ozone in the tropics. At levels below 550 K the air is influenced by midlatitude air which can be identified by N_2O values lower than the values of the middle- and high-latitude reference curves. The O_3/N_2O distribution in the tropics appears to be similar in both Hemispheres, seasonal changes are small and equal in both hemisphere. Similarly, as we find rather different characteristics for the O_3/N_2O distributions for the tropical, midlatitude, and polar regime, *Hudson et al.* [2003, 2006] report distinct and clearly separable temperature profiles (and thus tropopause heights), ozone profiles and total ozone values for the respective regimes.

[38] In the O_3/N_2O seasonal cycle for the midlatitudes (Figures 9 and 10) the air is centered around the May midlatitude and April high-latitude reference curves. The O_3/N_2O distribution is influenced by both high- and low-latitude air masses. In January (Figure 9a) and April (Figure 9b) the positive correlation at levels above 500 K is partly caused by tropical ozone production and partly by descent of polar air masses. Polar winter ozone loss is evident at 500 ± 25 K in January by an inflection of the curve as described in the previous section. In both hemispheres a seasonal dependence is visible.

[39] The seasonal dependence of the O_3/N_2O distribution and the differences between the hemispheres are most strongly pronounced in the seasonal cycle of monthly averaged N_2O and O_3 for the high latitudes (Figures 11 and 12). Thus, the separation into photochemical and dynamical processes can be most easily accomplished in

Midlatitude (SH)

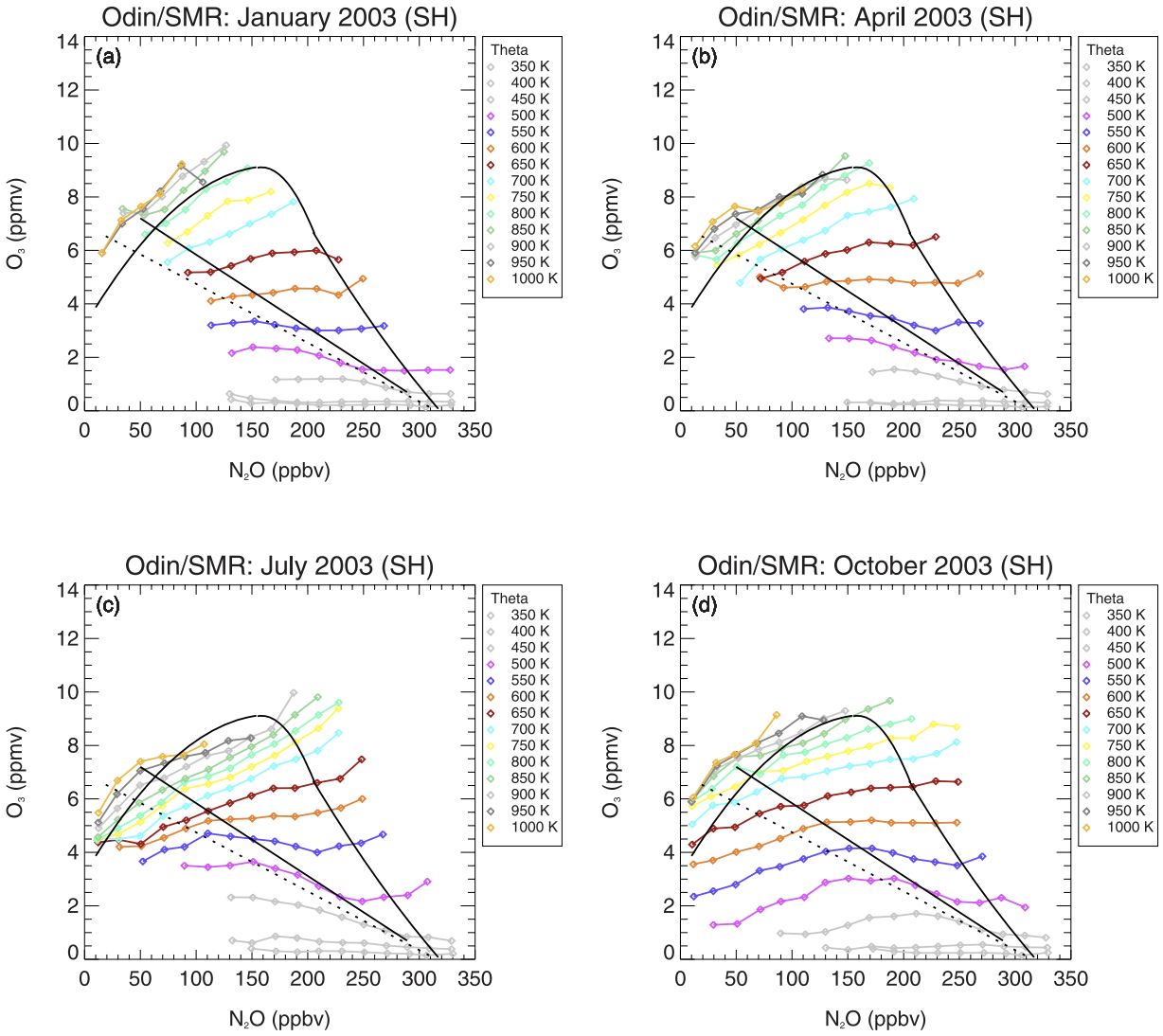

Figure 10. Southern Hemispheric monthly averaged N_2O and O_3 for the midlatitudes measured by Odin/SMR binned by potential temperature (Odin/SMR, 30–60°S). Additionally, the May midlatitude (ATMOS shuttle 1985, solid line), April high-latitude (ATMOS Shuttle 1993, dashed line), and November tropics (ATMOS Shuttle 1994, solid curve) reference curves are shown.

the polar regions. The most obvious difference is the signature of the Antarctic ozone hole noticeable by much lower ozone mixing ratios below 550 K in September (not shown) and October (Figure 12d) in the Southern Hemisphere and March (not shown) and April (Figure 12b) in the Northern Hemisphere [*Khosrawi et al.*, 2006]. Further, an important difference between the N_2O and O_3 distributions in the corresponding season is that diabatic descent, noticeable as a positive O_3/N_2O distribution at altitudes above 25 km (500 K), is much more pronounced in the Northern Hemisphere than in the Southern Hemisphere [e.g., *Shepherd*, 2003]. This difference is due to the fact that descent occurs earlier in the Southern Hemisphere than in the Northern Hemisphere and has a different balance with isentropic mixing [*Tuck and Proffitt*, 1997; *Tuck et al.*, 2002].

5.3. An Example for the Evaluation of Models

[40] Here, we will give an example how a model evaluation can be performed using the data set of monthly averaged N_2O and O_3 derived from Odin/SMR. For this purpose, using model data from KASIMA and CLaMS monthly averages of N_2O and O_3 were calculated as described in section 3 from these data sets. The CLaMS simulation used here was performed for the Arctic winter 2002/2003 [*Grooß et al.*, 2005]. The simulation started on 17 November 2002 and was run until 23 March 2003. The distributions of chemical species in the KASIMA simulation used here were initialized on 30 March 2002, with data from a long-term KASIMA run.

[41] To test whether the general characteristics of the CLaMS and KASIMA model results agree with Odin/

Polar (NH)

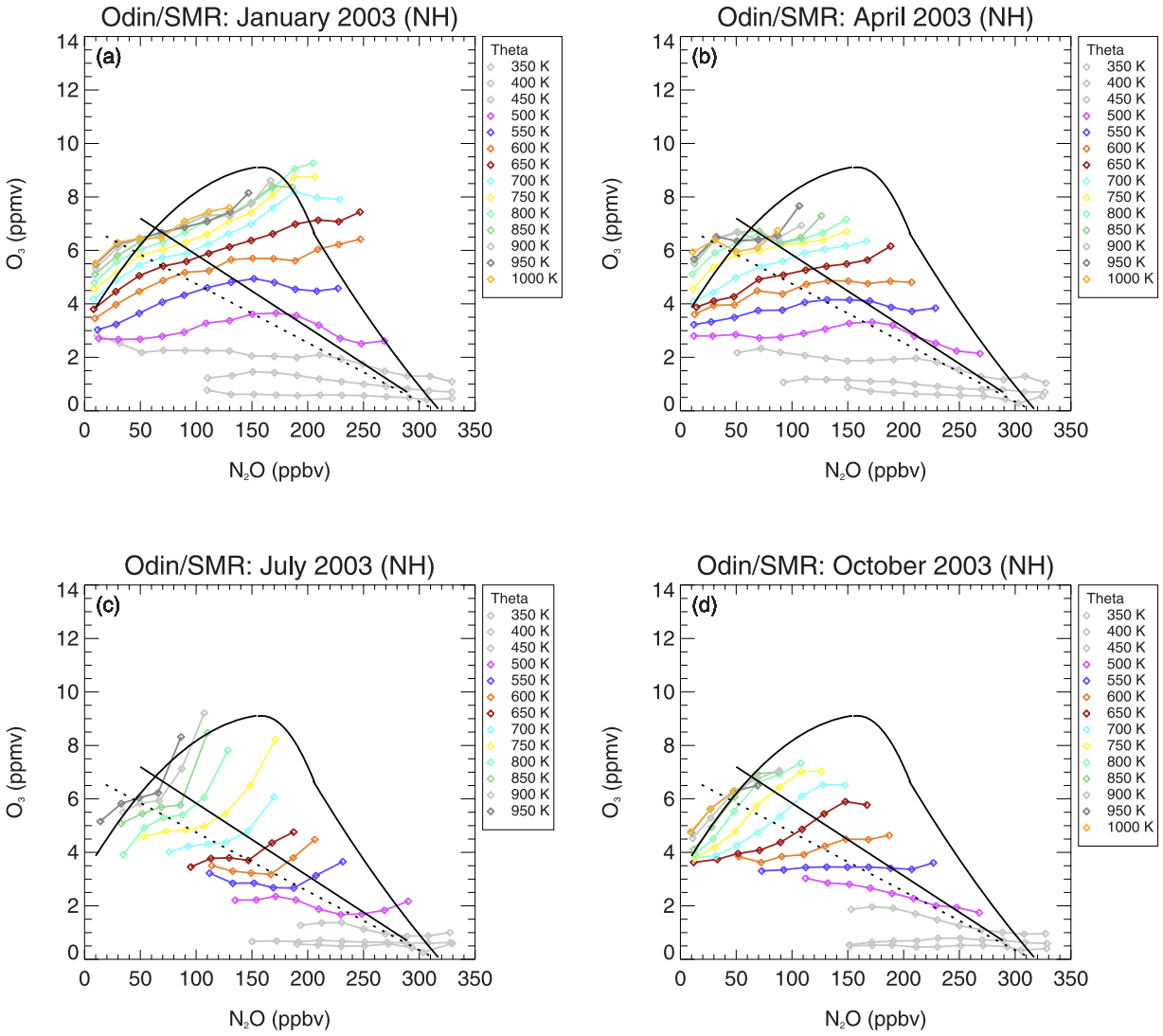

Figure 11. Northern Hemispheric monthly averaged N_2O and O_3 for the high latitudes measured by Odin/SMR binned by potential temperature (Odin/SMR, 60–90°N). Additionally, the May midlatitude (ATMOS Shuttle 1985, solid line), April high-latitude (ATMOS Shuttle 1993, dashed line), and November tropics (ATMOS Shuttle 1994, solid curve) reference curves are shown.

SMR measurements, figures analogous to Figure 3 were created (not shown). A good agreement between KASIMA and CLaMS with Odin/SMR was found with differences less than ±20%. For the evaluation the 500 K and 650 K potential temperature levels were chosen (Figure 13). The Odin/SMR data were taken as the reference (in gray diamonds). The differences between Odin/SMR and ILAS/ILAS-II, CLaMS and KASIMA are calculated as follows: D = [μ (Model) − μ (Odin)]/μ (Odin)*100 where μ denotes the O_3 mixing ratio at a given N_2O mixing ratio of the Odin/SMR measurement and model simulation, respectively.

[42] Figure 13 shows the evaluation for the Northern Hemisphere polar regions for February 2003. A good agreement between CLaMS, KASIMA, and ILAS/ILAS-II with Odin/SMR is found at 500 and 650 K. At 500 K all curves show the characteristic slope change from negative to positive correlated. While in the ILAS/ILAS-II and KASIMA averages the inflection is found at 170 ppbv N_2O, this inflection in CLaMS is found at somewhat higher N_2O mixing ratios, namely at 190 ppbv. While the absolute values of the O_3 averages of CLaMS and ILAS/ILAS-II agree quite well with Odin/SMR, the O_3 averages of KASIMA show somewhat higher values indicating that in the KASIMA simulation polar ozone loss possibly is slightly underestimated in February 2003.

[43] At 650 K all curves show the characteristic positive correlation which is caused by descent. CLaMS as well as KASIMA show a somewhat stronger positive correlation than is found in the Odin/SMR averages for N_2O mixing

Polar (SH)

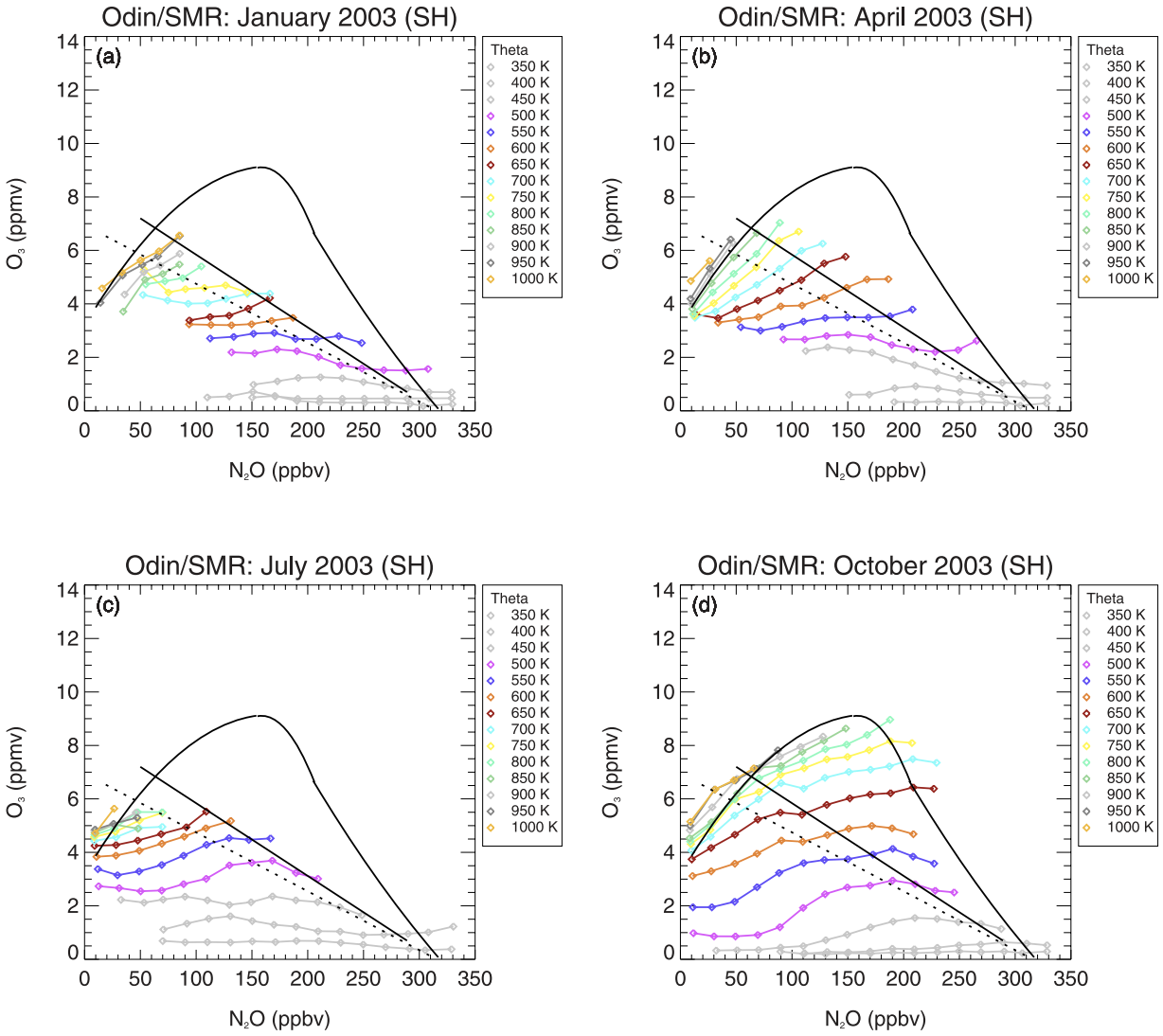

Figure 12. Southern Hemispheric monthly averaged N_2O and O_3 for the high latitudes measured by Odin/SMR binned by potential temperature (Odin/SMR, 60–90°S). Additionally, the May midlatitude (ATMOS Shuttle 1985, solid line), April high-latitude (ATMOS Shuttle 1993, dashed line), and November tropics (ATMOS Shuttle 1994, solid curve) reference curves are shown.

ratios greater than 150 ppbv. This stronger correlation could indicate that descent is slightly overestimated by the models or that mixing between midlatitude air and vortex air might be underestimated. The ILAS/ILAS-II averages are lower than Odin/SMR, CLaMS and KASIMA, which might be caused by differences in transport and chemistry between the winters 1996/1997 and 2002/2003. The ILAS/ILAS-II averages in February were derived from ILAS data measurements made in 1997.

[44] Both the CLaMS and KASIMA simulations used here show a good agreement with Odin/SMR. The differences between CLaMS, KASIMA and ILAS/ILAS-II, respectively, and Odin/SMR are generally less than ±20%. An extended evaluation study using CLaMS and KASIMA data will be presented in a separate study (Khosrawi et al., manuscript in preparation, 2008).

6. Conclusions

[45] The method by *Proffitt et al.* [2003] helps to reduce O_3 variability caused by transport processes by using averages of N_2O and O_3. Thereby, chemical and dynamical processes can be separated. Monthly averages of N_2O and O_3 were derived from ILAS/ILAS-II and Odin/SMR observations. Using the relationship between N_2O and potential temperature derived from ILAS/ILAS-II measurements we showed how the N_2O/O_3 distribution is influenced by diabatic descent. When descent is weak

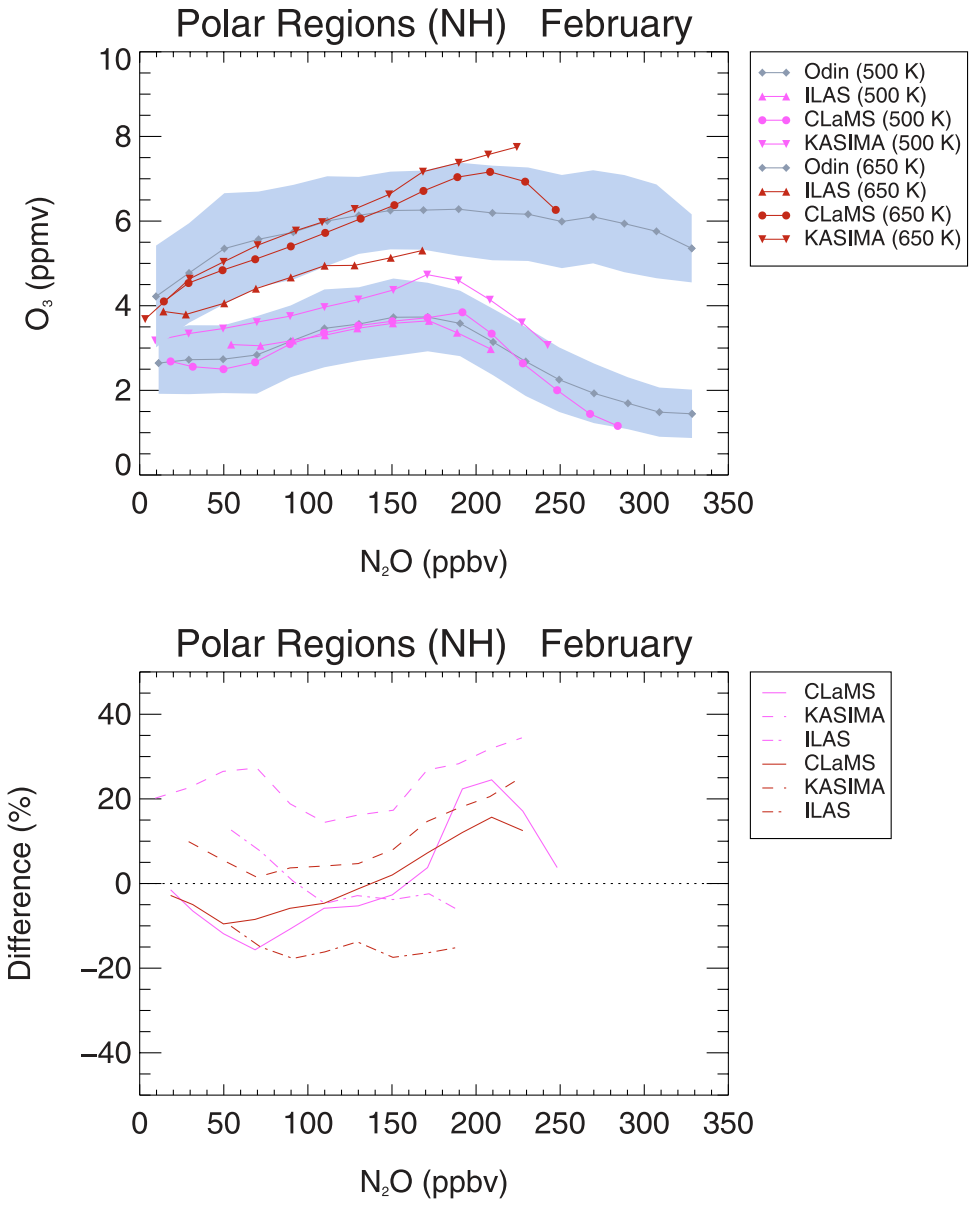

Figure 13. (top) Comparison of the monthly averages of N_2O and O_3 derived from CLaMS, KASIMA and ILAS/ILAS-II (colored curves) with Odin/SMR (gray) at 500 K and 650 K. The gray shaded area marks the range of Odin/SMR standard deviations of the averages. (bottom) Differences of the O_3 averages of CLaMS, KASIMA, and ILAS/ILAS-II from Odin/SMR.

an almost linear relationship is found between N_2O and potential temperature while when descent is strong a curved relationship is found. This relationship is reflected in the N_2O/O_3 distributions as follows. When descent is strong the N_2O/O_3 curves extend over a broader range of N_2O values and exhibit a positive correlation at potential temperature levels above 500 K. When descent is weak the N_2O/O_3 distribution is flat to negatively correlated at all potential temperature levels and a confinement of the N_2O/O_3 distribution to a smaller range of N_2O mixing ratios is found.

[46] The agreement of the ILAS/ILAS-II data set of monthly averaged N_2O and O_3 which we have derived in a previous study [*Khosrawi et al.*, 2006] with the Odin/SMR data set of monthly averaged N_2O and O_3 helps to verify our ILAS/ILAS-II data set and demonstrates that, at least in this case, limited sampling from satellite occultation instruments does not constitute a problem for our method. Further, a 1-year data set of monthly averaged N_2O and O_3 for the entire hemisphere was derived from Odin/SMR measurements as well as 1-year data sets of monthly averaged N_2O and O_3 for the low latitudes, midlatitudes and high latitudes. The 1-year data set of monthly averaged N_2O and O_3 derived from Odin/SMR shows that diabatic descent is to a certain extent masked by tropical ozone production when the entire hemisphere is considered. Thus, the separation into photochemical and dynamical processes can be most easily performed when only the polar regions are considered. However, our 1-year data sets of monthly averaged N_2O

and O_3 for the two hemispheres allow us to investigate the seasonal cycle of N_2O/O_3 on a global scale. Moreover, the separation of the data sets of monthly averaged N_2O and O_3 into high, middle and low latitudes allows us to investigate the seasonal cycle of the N_2O/O_3 distribution in each hemisphere and latitude region. Thereby, we found that the seasonal dependence and differences in the hemispheres are most pronounced in the polar regions. In contrast, the tropical regions change little from season to season, and between hemispheres. These data sets of monthly averaged N_2O and O_3 provide a potentially important tool for the evaluation of atmospheric photochemical models like CTMs and GCMs. An example how such an evaluation study can be performed was given by using model results of two CTMs, namely the CLaMS and KASIMA model. A good agreement between Odin/SMR and the CTMs CLaMS and KASIMA is found with differences generally less than ±20%. An extended evaluation study using CLaMS and KASIMA, as well as other models, will be presented in a separate study (Khosrawi et al., manuscript in preparation, 2008).

[47] **Acknowledgments.** The Improved Limb Atmospheric Spectrometer (ILAS and ILAS-II) were developed by the Ministry of the Environment of Japan. The ILAS and ILAS-II data were processed at the ILAS/ILAS-II Data Handling Facility, National Institute of Environmental Studies (NIES), Japan. A part of this work was supported by the Global Environment Research Fund provided by the Ministry of the Environment of Japan (MOE). We are grateful to P. Ricaud and J. de La Noë of the Observatoire de Bordeaux and to C. Boone of the Service d'Aéronomie, Paris, for their kind assistance in providing Odin/SMR data through the French atmospheric database ETHER (http://ether.ipsl.jussieu.fr/). Odin is a Swedish-led satellite project funded jointly by Sweden (SNSB), Canada (CSA), Finland (TEKES), and France (CNES). We are also grateful to the anonymous referees for their helpful comments, to M. von Hobe and K. Waigel for programming support, and to the European Commission for funding F. Khosrawi by the EU 6th Framework Programme–Marie-Curie Intra-European Fellowships.

References

Anderson, J. G., W. H. Brune, and M. H. Proffitt (1989), Ozone destruction by chlorine radicals within the Antarctic vortex—The spatial and temporal evolution of ClO-O_3 anticorrelation based on in situ ER-2 data, *J. Geophys. Res.*, *94*, 11,465–11,479.

Bacmeister, J. T., M. R. Schoeberl, M. E. Summers, J. R. Rosenfield, and X. Zhu (1995), Descent of long-lived trace gases in the winter polar vortex, *J. Geophys. Res.*, *100*, 11,669–11,684.

Bauer, R., A. Engel, H. Franken, E. Klein, G. Kulessa, C. Schiller, and U. Schmidt (1994), Monitoring the vertical structure of the Arctic polar vortex over northern Scandinavia during EASOE: Regular N_2O profile observations, *Geophys. Res. Lett.*, *21*, 1211–1214.

Bian, H., and M. Prather (2002), Fast-J2: Accurate simulation of stratospheric photolysis in global chemical models, *J. Atmos. Chem.*, *41*, 281–296.

Browell, E. V., et al. (1990), Airborne LIDAR observations in the wintertime Arctic stratosphere: Ozone, *Geophys. Res. Lett.*, *17*, 325–328.

Crutzen, P. J. (1970), The influence of nitrogen oxides on the atmospheric ozone content, *Q.J.R. Meteorol. Soc.*, *96*, 320–325.

Crutzen, P. J., and C. Brühl (2001), Catalysis by NOx as the main cause of the spring to fall stratospheric ozone decline in the Northern Hemisphere, *J. Phys. Chem. A*, *105*, 1579–1582.

Danielsen, E. F., and H. Houben (1988), Dynamics of the Antarctic stratosphere and implications for the ozone hole, in *Anthropogene Beeinflussung der Ozonschicht*, pp. 191–242, DECHEMA, Frankfurt, Germany.

Ejiri, M. K., et al. (2006), Validation of ILAS-II V1.4 nitrous oxide and methane profiles, *J. Geophys. Res.*, *111*, D22S90, doi:10.1029/2005JD006449.

Engel, A., et al. (2006), Observation of mesospheric air inside the Arctic stratospheric polar vortex in early 2003, *Atmos. Chem. Phys.*, *6*, 267–282.

Eyring, V., et al. (2006), Assessment of temperature, trace species and ozone in chemistry-climate simulations of the recent past, *J. Geophys. Res.*, *111*, D22308, doi:10.1029/2006JD007327.

Fahey, D. W., S. Solomon, S. R. Kawa, M. Loewenstein, J. R. Podolske, S. E. Strahan, and K. R. Chan (1990), A diagnostic for denitrification in the winter polar stratospheres, *Nature*, *345*, 698–702.

Farman, J. C., B. G. Gardiner, and J. D. Shanklin (1985a), Large losses of total ozone in Antarctica reveal seasonal ClO_x/NO_x interaction, *Nature*, *315*, 207–210.

Farman, J. C., R. J. Murgatroyd, A. M. Silnickas, and B. A. Thrush (1985b), Ozone photochemistry in the Antarctic stratosphere in summer, *Q.J.R. Meteorol. Soc.*, *111*, 1013–1025.

Frisk, U., et al. (2003), The Odin satellite: I. Radiometer design and test, *Astron. Astrophys.*, *403*(3), 27–34.

Goutail, F., et al. (2005), Early unusual ozone loss during the Arctic winter 2002/2003 compared to other winters, *Atmos. Chem. Phys.*, *5*, 665–677.

Greenblatt, J. B., et al. (2002), Tracer-based determination of vortex descent in the 1999/2000 Arctic winter, *J. Geophys. Res.*, *107*(D20), 8279, doi:10.1029/2001JD000937.

Grooß, J.-U., and J. M. Russell (2005), Technical note: A stratospheric climatology for O_3, H_2O, CH_4, NO_x, HCl and HF derived from HALOE measurements, *Atmos. Chem. Phys.*, *5*, 2797–2807.

Grooß, J.-U., G. Günther, R. Müller, P. Konopka, S. Bausch, H. Schlager, C. Voigt, C. M. Volk, and G. C. Toon (2005), Simulation of denitrification and ozone loss for the Arctic winter 2002/2003, *Atmos. Chem. Phys.*, *5*, 1437–1448.

Hegglin, M. I., and T. G. Shepherd (2007), O_3-N_2O correlations from the Atmospheric Chemistry Experiment: Revisiting a diagnostic of transport and chemistry in the stratosphere, *J. Geophys. Res.*, *112*, D19301, doi:10.1029/2006JD008281.

Hudson, R. D., A. D. Frolov, M. F. Andrade, and M. B. Folette (2003), The total ozone field separated into meteorological regimes. Part I: Defining the regimes, *J. Atmos. Sci.*, *60*, 1669–1677.

Hudson, R. D., M. F. Andrade, M. B. Folette, and A. D. Frolov (2006), The total ozone field separated into meteorological regimes—Part II: Northern Hemisphere mid-latitude total ozone trends, *Atmos. Chem. Phys.*, *6*, 5183–5191.

Johnston, H. S. (1975), Global ozone balance in the natural stratosphere, *Rev. Geophys.*, *13*, 637–649.

Kanzawa, H., et al. (2002), Validation and data characteristics of water vapor profiles observed by the Improved Limb Atmospheric Spectrometer (ILAS) and processed with the version 5.20 algorithm, *J. Geophys. Res.*, *107*(D24), 8217, doi:10.1029/2001JD000881. (Correction, *J. Geophys. Res.*, 108 (D4), 8218, doi:10.1029/20003JD001601, 2003.)

Kawamoto, N., H. Kanzawa, and M. Shiotani (2004), Time variations of descent in the Antarctic vortex during the early winter of 1997, *J. Geophys. Res.*, *109*, D18309, doi:10.1029/2004JD004650.

Kelly, K. K., et al. (1989), Dehydration in the lower Antarctic stratosphere during late winter and early spring, 1987, *J. Geophys. Res.*, *94*, 11,317–11,357.

Khosrawi, F., R. Müller, M. H. Proffitt, and H. Nakajima (2004), Monthly averaged ozone and nitrous oxide from the Improved Limb Atmospheric Spectrometer (ILAS) in the Northern and Southern Hemisphere polar regions, *J. Geophys. Res.*, *109*, D10301, doi:10.1029/2003JD004365.

Khosrawi, F., R. Müller, M. H. Proffitt, and H. Nakajima (2006), Monthly averages of nitrous oxide and ozone for the Northern and Southern Hemisphere high latitudes: A "1-year climatology" derived from ILAS/ILAS-II observations, *J. Geophys. Res.*, *111*, D11S11, doi:10.1029/2005JD006384.

Konopka, P., et al. (2004), Mixing and ozone loss in the 1999–2000 Arctic vortex: Simulations with the three-dimensional Chemical Lagrangian Model of the Stratosphere CLaMS, *J. Geophys. Res.*, *109*, D02315, doi:10.1029/2003JD003792.

Kouker, W., I. Langbein, T. Reddmann, and R. Ruhnke (1999), The Karlsruhe Simulation Model of the Middle Atmosphere (KASIMA), Version 2, *Tech. Rep. 6278*, Inst. für Meteorol. und Klimaforsch., Forschungszent. Karlsruhe, Karlsruhe, Germany.

Kuttipurath, J., et al. (2007), Intercomparison of ozone profile measurements from ASUR, SCIAMACHY, MIPAS, OSIRIS, and SMR, *J. Geophys. Res.*, *112*, D09311, doi:10.1029/2006JD007830.

Lemmen, C., R. Müller, P. Konopka, and M. Dameris (2006), Critique of the tracer-tracer correlation technique and its potential to analyse polar ozone loss in chemistry-climate models, *J. Geophys. Res.*, *111*, D18307, doi:10.1029/2006JD007298.

Llewellyn, E. J., et al. (2004), The OSIRIS instrument on the Odin spacecraft, *Can. J. Phys.*, *82*, 411–422.

McIntyre, M. E. (1992), Atmospheric dynamics: Some fundamentals, with observational implications, *Proc. Int. Sch. Phys. Enrico Fermi*, *CXV*, 313–386.

McKenna, D. S., et al. (1990), Calculations of ozone destruction during the 1988/89 Arctic winter, *Geophys. Res. Lett.*, *17*, 553–556.

McKenna, D. S., P. Konopka, J.-U. Grooß, G. Günther, R. Müller, R. Spang, D. Offermann, and Y. Orsolini (2002a), A new Chemical Lagrangian Model of the Stratosphere (CLaMS): 1. Formulation of advection and mixing, *J. Geophys. Res.*, *107*(D16), 4309, doi:10.1029/2000JD000114.

McKenna, D. S., J.-U. Grooß, G. Günther, P. Konopka, R. Müller, G. Carver, and Y. Sasano (2002b), A new Chemical Lagrangian Model of the Stratosphere (CLaMS): 2. Formulation of chemistry-scheme and initialisation, *J. Geophys. Res.*, *107*(D15), 4256, doi:10.1029/2000JD000113.

Merino, F., D. P. Murtagh, M. Ridal, J. E. P. Eriksson, P. Baron, P. Ricaud, and J. De La Noë (2002), Studies on the Odin sub-millimetre radiometer: III. Performance simulations, *Can. J. Phys.*, *80*(4), 357–373.

Michelsen, H. A., G. L. Manney, M. R. Gunson, and R. Zander (1998), Correlations of stratospheric abundances of NO_y, O_3, N_2O, and CH_4 derived from ATMOS measurements, *J. Geophys. Res.*, *103*, 28,347–28,359.

Morcrette, J.-J. (1991), Radiation and cloud radiative properties in the European Centre for Medium Range Weather Forecasts forecasting system, *J. Geophys. Res.*, *96*, 9121–9132.

Müller, R., P. J. Crutzen, J.-U. Grooß, C. Brühl, J. M. Russel III, and A. F. Tuck (1996), Chlorine activation and ozone depletion in the Arctic vortex: Observations by the Halogen Occultation Experiment on the Upper Atmosphere Research Satellite, *J. Geophys. Res.*, *101*, 12,531–12,554.

Müller, R., et al. (2007), Impact of mesospheric intrusions on ozone-tracer relations in the stratospheric polar vortex, *J. Geophys. Res.*, *112*, D23307, doi:10.1029/2006JD008315.

Murphy, D. M. (1991), Ozone loss rates calculated along ER-2 flight tracks, *J. Geophys. Res.*, *96*, 5045–5053.

Murphy, D. M., A. F. Tuck, K. K. Kelly, K. R. Chan, M. Loewenstein, J. R. Podolske, M. H. Proffitt, and S. E. Strahan (1989), Indicators of transport and vertical motion from correlations between in-situ measurements in the Airborne Anarctic Ozone Experiment, *J. Geophys. Res.*, *94*, 11,669–11,685.

Murtagh, D., et al. (2002), An overview of the Odin atmospheric mission, *Can. J. Phys.*, *80*(4), 309–319.

Nakajima, H., et al. (2006a), Characteristics and performance of the Improved Limb Atmospheric Spectrometer-II (ILAS-II) on board the ADEOS-II satellite, *J. Geophys. Res.*, *111*, D11S01, doi:10.1029/2005JD006334.

Nakajima, H., et al. (2006b), Measurements of $ClONO_2$ by the Improved Limb Atmospheric Spectrometer (ILAS) in high latitude stratosphere: New products of version 6.1 data processing, *J. Geophys. Res.*, *111*, D11S09, doi:10.1029/2005JD006441.

Perliski, L. S., S. Solomon, and J. London (1989), On the interpretation of seasonal variations of stratospheric ozone, *Planet. Space Sci.*, *37*, 1527–1538.

Pierce, R. B., T. D. Fairlie, E. E. Remsberg, J. M. Russell, and W. L. Grose (1997), HALOE observations of the Arctic vortex during the 1997 spring: Horizontal structure in the lower stratosphere, *Geophys. Res. Lett.*, *24*, 2701–2704.

Pierce, R. B., J. A. Al-Saadi, T. D. Fairlie, J. R. Olson, R. S. Eckman, G. S. Lingenfelser, W. L. Grose, and J. M. Russell (1999), Large-scale stratospheric ozone photochemistry and transport during the POLARIS campaign, *J. Geophys. Res.*, *104*, 26,525–26,545.

Plumb, R. A., and M. K. W. Ko (1992), Interrelationships between mixing ratios of long-lived stratospheric constituents, *J. Geophys. Res.*, *97*, 10,145–10,156.

Plumb, R. A., W. Heres, J. L. Neu, N. Mahowald, J. del Corral, G. C. Toon, E. Ray, F. L. Moore, and A. E. Andrews (2002), Global tracer modeling during SOLVE: High-latitude descent and mixing, *J. Geophys. Res.*, *107*, 8309, doi:10.1029/2001JD001023 [printed *108* (D5), 2003].

Proffitt, M. H., D. Fahey, K. Kelly, and A. Tuck (1989a), High latitude ozone loss outside the Antarctic ozone hole, *Nature*, *342*, 233–237.

Proffitt, M. H., K. K. Kelly, J. A. Powell, B. L. Gary, M. Loewenstein, J. R. Podolske, S. E. Strahan, and K. R. Chan (1989b), Evidence of diabatic cooling and poleward transport within and around the 1987 Antarctic Ozone Hole, *J. Geophys. Res.*, *94*, 16,797–16,813.

Proffitt, M. H., et al. (1989c), A chemical definition of the boundary of the Antarctic ozone hole, *J. Geophys. Res.*, *94*, 11,437–11,448.

Proffitt, M. H., et al. (1989d), In-situ measurements within the 1987 Antarctic ozone hole from a high-altitude ER-2 aircraft, *J. Geophys. Res.*, *94*, 16,547–16,555.

Proffitt, M. H., J. J. Margitan, K. K. Kelly, M. Loewenstein, J. R. Podolske, and K. R. Chan (1990), Ozone loss in the Arctic polar vortex inferred from high altitude aircraft measurements, *Nature*, *347*, 31–36.

Proffitt, M. H., K. Aikin, J. J. Margitan, M. Loewenstein, J. R. Podolske, A. Weaver, K. R. Chan, H. Fast, and J. W. Elkins (1993), Ozone loss inside the northern polar vortex during the 1991–1992 winter, *Science*, *261*, 1150–1154.

Proffitt, M. H., K. Aikin, A. F. Tuck, J. J. Margitan, C. R. Webster, G. C. Toon, and J. W. Elkins (2003), Seasonally averaged ozone and nitrous oxide in the Northern Hemisphere lower stratosphere, *J. Geophys. Res.*, *108*(D3), 4110, doi:10.1029/2002JD002657.

Randel, W. J., J. C. Gille, A. E. Roche, J. B. Kumer, J. L. Mergenthaler, J. W. Waters, E. F. Fishbein, and W. A. Lahoz (1993), Stratospheric transport from the tropics to middle latitudes by planetary-wave mixing, *Nature*, *365*, 533–535.

Ray, E. A., F. L. Moore, J. W. Elkins, D. F. Hurst, P. A. Romashkin, G. S. Dutton, and D. W. Fahey (2002), Descent and mixing in the 1999–2000 northern polar vortex inferred from in situ tracer measurements, *J. Geophys. Res.*, *107*(D20), 8285, doi:10.1029/2001JD000961.

Reddmann, T., R. Ruhnke, and W. Kouker (2001), Three-dimensional model simulations of SF6 with mesospheric chemistry, *J. Geophys. Res.*, *106*, 14,525–14,537.

Rex, M., et al. (1999), Subsidence, mixing and denitrification of Arctic polar vortex air measured during POLARIS, *J. Geophys. Res.*, *104*, 26,611–26,623.

Rosenfield, J. E., P. A. Newman, and M. R. Schoeberl (1994), Computations of diabatic descent in the stratospheric polar vortex, *J. Geophys. Res.*, *99*(D8), 16,677–16,689.

Ruhnke, R., W. Kouker, and T. Reddmann (1999), The influence of the OH + NO_2 + M reaction on the NO_y partitioning in the late arctic winter 1992/1993 as studied with KASIMA, *J. Geophys. Res.*, *104*, 3755–3772.

Russell, J. M., L. L. Gordley, J. H. Park, S. R. Drayson, A. F. Tuck, J. E. Harries, R. J. Cicerone, P. J. Crutzen, and J. E. Frederick (1993a), The Halogen Occultation Experiment, *J. Geophys. Res.*, *98*, 10,777–10,797.

Russell, J. M., A. F. Tuck, L. L. Gordley, J. H. Park, S. R. Drayson, J. E. Harries, R. J. Cicerone, and P. J. Crutzen (1993b), HALOE Antarctic observations in spring 1991, *Geophys. Res. Lett.*, *20*, 719–722.

Salawitch, R., et al. (1990), Loss of ozone in the Arctic vortex for the winter of 1989, *Geophys. Res. Lett.*, *17*, 561–564.

Salawitch, R., et al. (2002), Chemical loss of ozone during the Arctic winter of 1999–2000: An analysis based on balloon-borne observations, *J. Geophys. Res.*, *107*(D20), 8269, doi:10.1029/2001JD000620.

Sander, S. P., et al. (2003), Chemical kinetics and photochemical data for the use in atmospheric studies, evaluation 14, *JPL Publ. 02–25*, NASA Jet Propul. Lab., Pasadena, Calif.

Sankey, D., and T. G. Shepherd (2003), Correlation of long-lived chemical species in a middle atmosphere general circulation model, *J. Geophys. Res.*, *108*(D16), 4494, doi:10.1029/2002JD002799.

Sasano, Y., M. Suzuki, T. Yokota, and H. Kanzawa (1999), Improved Limb Atmospheric Spectrometer (ILAS) for stratospheric ozone layer measurements by solar occultation technique, *Geophys. Res. Lett.*, *26*, 197–200.

Schoeberl, M. R., and D. L. Hartmann (1991), The dynamics of the stratospheric polar vortex and its relation to springtime ozone depletions, *Science*, *251*, 46–52.

Shepherd, T. G. (2003), Large-scale atmospheric dynamics for atmospheric chemists, *Chem. Rev.*, *103*(12), 4509–4532, doi:10.1021/cr020511z.

Solomon, S., J. T. Kiehl, R. R. Garcia, and W. Grose (1986), Tracer transport by the diabatic circulation deduced from satellite observations, *J. Atmos. Sci.*, *43*, 1603–1617.

Strahan, S., M. Loewenstein, and J. Podolske (1999), Climatology and small-scale structure of lower stratospheric N_2O based on in-situ observations, *J. Geophys. Res.*, *104*, 2195–2208.

Sugita, T., et al. (2002), Validation of ozone measurements from the Improved Limb Atmospheric Spectrometer (ILAS), *J. Geophys. Res.*, *107*(D24), 8212, doi:10.1029/2001JD000602.

Sugita, T., et al. (2006), A comparative study of ozone profiles in the stratosphere and the lower mesosphere measured by the Improved Limb Atmospheric Spectrometer (ILAS-II), ozonsondes, and satellite profiles, *J. Geophys. Res.*, *111*, D11S02, doi:10.1029/2005JD006439.

Swinbank, R., and A. O'Neill (1994), A stratosphere-troposphere data assimilation system, *Mon. Weather Rev.*, *122*, 686–702.

Tilmes, S., R. Müller, J.-U. Grooß, M. Höpfner, G. C. Toon, and J. M. Russell (2003a), Very early chlorine activation and ozone loss in the Arctic winter 2002–2003, *Geophys. Res. Lett.*, *30*(23), 2201, doi:10.1029/2003GL018079.

Tilmes, S., R. Müller, J.-U. Grooß, D. S. McKenna, J. M. Russell, and Y. Sasano (2003b), Calculation of chemical ozone loss in the Arctic winter 1996–1997 using ozone-tracer correlations: Comparison of Improved Limb Atmospheric Spectrometer (ILAS) and Halogen Occultation (HALOE) results, *J. Geophys. Res.*, *108*(D2), 4045, doi:10.1029/2002JD002213.

Tilmes, S., R. Müller, J.-U. Grooß, and J. M. Russell (2004), Ozone loss and chlorine activation in the Arctic winters 1991–2003 derived with the tracer-tracer correlations, *Atmos. Chem. Phys.*, *4*, 2181–2213.

Tilmes, S., R. Müller, J.-U. Grooß, H. Nakajima, and Y. Sasano (2006a), Development of tracer-tracer correlations and chemical ozone loss during the setup phase of the polar vortex, *J. Geophys. Res.*, *111*, D24S90, doi:10.1029/2005JD006726.

Tilmes, S., R. Müller, J.-U. Grooß, R. Spang, H. Nakajima, and Y. Sasano (2006b), Chemical ozone loss and related processes in the Antarctic winter 2003 based on ILAS-II observations, *J. Geophys. Res.*, *111*, D11S12, doi:10.1029/2005JD006260.

Tilmes, S., D. Kinnison, R. Müller, F. Sassi, D. R. Marsh, B. A. Boville, and R. Garcia (2007), Evaluation of heterogeneous processes in the polar lower stratosphere in the Whole Atmosphere Community Climate Model, *J. Geophys. Res.*, *112*, D24301, doi:10.1029/2006JD008334.

Toon, G. C., J.-F. Blavier, B. Sen, R. J. Salawitch, G. B. Osterman, J. Notholt, M. Rex, C. T. McElroy, and J. M. Russell III (1999), Ground-based observations of Arctic O_3 loss during spring and summer 1997, *J. Geophys. Res.*, *104*, 26,497–26,510.

Tuck, A. F. (1989), Synoptic and chemical evolution of the Antarctic vortex in late winter and early spring, 1987, *J. Geophys. Res.*, *94*, 11,687–11,737.

Tuck, A. F., and M. H. Proffitt (1997), Comment on "On the magnitude of transport out of the Antarctic polar vortex" by Wiel M. F. Wauben et al., *J. Geophys. Res.*, *102*, 28,215–28,218.

Tuck, A. F., K. K. Kelly, C. R. Webster, M. Loewenstein, R. M. Stimpfle, M. H. Proffitt, and K. R. Chan (1995), Airborne chemistry and dynamics at the edge of the 1994 Antarctic vortex, *J. Chem. Soc. Faraday Trans.*, *91*, 3063–3071.

Tuck, A. F., S. J. Hovde, E. C. Richard, D. W. Fahey, R. S. Gao, and T. P. Bui (2002), A scaling analyses of ER-2 data in the inner Arctic vortex during January–March 2000, *J. Geophys. Res.*, *107*, 8306, doi:10.1029/2001JD000879 [printed *108* (D5), 2003].

Urban, J., et al. (2004), The Northern Hemisphere stratospheric vortex during the 2002–03 winter: Subsidence, chlorine activation and ozone loss observed by the Odin Sub-Millimetre Radiometer, *Geophys. Res. Lett.*, *31*, L07103, doi:10.1029/2003GL019089.

Urban, J., et al. (2005a), Odin/SMR limb observations of stratospheric trace gases: Validation of N_2O, *J. Geophys. Res.*, *110*, D09301, doi:10.1029/2004JD005394.

Urban, J., et al. (2005b), Odin/SMR limb observations of stratospheric trace gases: Level 2 processing of ClO, N_2O, HNO_3, and O_3, *J. Geophys. Res.*, *110*, D14307, doi:10.1029/2004JD005741.

Volk, C. M., et al. (1996), Quantifying transport between the tropical and mid-latitude lower stratosphere, *Science*, *272*, 1763–1768.

Volk, C. M., J. W. Elkins, D. W. Fahey, G. S. Dutton, J. M. Gilligan, M. Loewenstein, J. R. Podolske, and K. R. Chan (1997), On the evaluation of source gas lifetimes from stratospheric observations, *J. Geophys. Res.*, *102*, 25,543–25,564.

Waugh, D. W., et al. (1997), Mixing of polar vortex air into middle latitudes as revealed by tracer-tracer scatterplots, *J. Geophys. Res.*, *102*, 13,119–13,134.

Yokota, T., et al. (2002), Improved Limb Atmospheric Spectrometer (ILAS) data retrieval algorithm for Version 5.20 gas profile products, *J. Geophys. Res.*, *107*(D24), 8216, doi:10.1029/2001JD000628.

J.-U. Grooß and R. Müller, ICG-1: Stratosphere, Forschungszentrum Jülich, D-52425 Jülich, Germany. (j.-u.grooss@fz-juelich.de; ro.mueller@fz-juelich.de)

F. Khosrawi, Department of Applied Environmental Science, Stockholm University, SE-10691 Stockholm, Sweden. (farah@misu.su.se)

D. Murtagh and J. Urban, Department of Radio and Space Science, Chalmers University of Technology, SE-41296 Göteborg, Sweden. (donal@rss.chlamers.se; jo.urban@rss.chalmers.se)

H. Nakajima, Ozone Layer Research Project, National Institute for Environmental Studies, 16-2 Onogawa, Tsukuba, Ibaraki 305-8506, Japan. (nakajima@nies.go.jp)

M. H. Proffitt, Proffitt Instruments Inc., Cabildo 480 UF 333, General Pacheco, Buenos Aires 1617, Argentina. (proffitt@uolsinectis.com.ar)

R. Ruhnke, Institute for Meteorology and Climate Research, Forschungszentrum Karlsruhe, D-76021 Karlsruhe, Germany. (r.ruhnke@imk.fzk.de)